Technical Report Documentation Page

1. Report No. FHWA/TX-11/0-6005-1	2. Government Accession No.	3. Recipient's Catalog No.
4. Title and Subtitle Progress During the First Year Towards Building the Total Pavement Acceptance Device (TPAD)		5. Report Date February 2010; Revised August 2010 6. Performing Organization Code
7. Author(s) Kenneth H. Stokoe, II, Loukas F. Kallivokas, Boo H. Nam, Claire K. Carpenter, Adam D. Bryant, Damon A. Weeks, Joseph H. Beno (CTR); Thomas Scullion, and Wenting Liu (TTI)		8. Performing Organization Report No. 0-6005-1
9. Performing Organization Name and Address Center for Transportation Research The University of Texas at Austin 1616 Guadalupe, Ste. 4.202 Austin, TX 78701-1255 Texas Transportation Institute Texas A&M University System 3135 TAMU College Station, Texas 77843-3135		10. Work Unit No. (TRAIS) 11. Contract or Grant No. 0-6005
12. Sponsoring Agency Name and Address Texas Department of Transportation Research and Technology Implementation Office P.O. Box 5080 Austin, TX 78763-5080		13. Type of Report and Period Covered Annual Report; 9/1/2008-8/31/2009 14. Sponsoring Agency Code
15. Supplementary Notes Project performed in cooperation with the Texas Department of Transportation and the Federal Highway Administration. Project Title: Developing a Testing Device for Total Pavements Acceptance		
16. Abstract During the first year of Project 0-6005, significant progress was made towards developing the Total Pavement Acceptance Device (TPAD). The TPAD will be a multi-function device that will be used to survey continuously along pavements at speeds in the range of 5 to 10 mph. The test functions will include those associated with Rolling Dynamics Deflectometer (RDD), ground penetrating radar (GPR), DMI and high-precision differential GPS, and surface temperature measurements, as well as digital video imaging of the pavement and right-of-way conditions. The basic moving platform for the TPAD was selected and initial prototype tests were conducted at the TxDOT Flight Services Facility at ABIA. Progress was made in developing: (1) improved rolling sensors and associated data analysis methods commensurate with the target testing speeds and (2) an integrated data acquisition and display system that records all test functions on the same time and distance baselines.		
17. Key Words Continuous Deflection Profiling, Testing Speed, GPR and GPS Measurements, Video Imaging, Single Moving Platform	18. Distribution Statement No restrictions. This document is available to the public through the National Technical Information Service, Springfield, Virginia 22161; www.ntis.gov.	

19. Security Classif. (of report)	20. Security Classif. (of this page)	21. No. of pages	22. Price
Unclassified	Unclassified	80	

Form DOT F 1700.7 (8-72) Reproduction of completed page authorized

Progress during the First Year towards Building the Total Pavement Acceptance Device (TPAD)

CTR
Kenneth H. Stokoe, II
Loukas F. Kallivokas
Boo H. Nam
Claire K. Carpenter
Adam D. Bryant
Damon A. Weeks
Joseph H. Beno

TTI
Thomas Scullion
Wenting Liu TTI

CTR Technical Report:	0-6005-1
Report Date:	February 2010; Revised August 2010
Project:	0-6005
Project Title:	Developing a Testing Device for Total Pavements Acceptance
Sponsoring Agency:	Texas Department of Transportation
Performing Agency:	Center for Transportation Research at The University of Texas at Austin

Project performed in cooperation with the Texas Department of Transportation and the Federal Highway Administration.

Center for Transportation Research
The University of Texas at Austin
1616 Guadalupe, Ste. 4.202
Austin, TX 78701-1255

www.utexas.edu/research/ctr

Disclaimers

Author's Disclaimer: The contents of this report reflect the views of the authors, who are responsible for the facts and the accuracy of the data presented herein. The contents do not necessarily reflect the official view or policies of the Federal Highway Administration or the Texas Department of Transportation (TxDOT). This report does not constitute a standard, specification, or regulation.

Patent Disclaimer: There was no invention or discovery conceived or first actually reduced to practice in the course of or under this contract, including any art, method, process, machine manufacture, design or composition of matter, or any new useful improvement thereof, or any variety of plant, which is or may be patentable under the patent laws of the United States of America or any foreign country.

Engineering Disclaimer

NOT INTENDED FOR CONSTRUCTION, BIDDING, OR PERMIT PURPOSES.

Project Engineer: Kenneth H. Stokoe, II
Professional Engineer License State and Number: Texas No. 49095
P. E. Designation: Research Supervisor

Acknowledgments

The research team wishes to express its sincere gratitude to TxDOT for supporting this research project. The interaction and support from the Research Monitoring Committee—Mr. Joe Leidy, Mr. Ed Oshinski, Dr. Dar Hao Chen and Dr. German Claros—has been very important to the progress of the project. The UT Staff—Mr. Cecil Hoffpauir, Mr. Curtis Mullins, and Dr. Farn-Yuh Menq, and graduate student Mr. Jung Su Lee—helped significantly in the field tests with the UT RDD and prototype ivi RDD. We owe much to Industrial Vehicles Incorporated (ivi) for developing the prototype ivi RDD. The generosity of Mr. Jay Bird, Mr. Elmo Christensen, and Mr. Mike Grady of ivi in sharing their ideas and the prototype vehicle with us, at no cost to the project, is greatly appreciated. Performance studies and a feasibility analysis of adapting a vehicle like the one built by ivi to act as the moving platform of the TPAD and to perform the RDD functions would have involved much speculation without the prototype vehicle. Finally, we are grateful to Mr. Don Ramsey and the personnel of the TxDOT Flight Services Facility for their kindness in allowing us to develop and use a pavement testbed at their facility.

Table of Contents

List of Figures

List of Tables

Chapter 1. Introduction

1.1 Project Objectives and Overview

The primary objective of Project 0-6005 is to develop a new nondestructive testing device that will be used to assess pavement structural conditions "on the fly." The device is presently called the Total Pavement Acceptance Device (TPAD). The TPAD will be a multi-function device that will be used to continuously survey the pavements at speeds in the range of 5 to 10 mph. The test functions will include those associated with Rolling Dynamic Deflectometer (RDD), ground penetrating radar (GPR), Distance Measurement Instrument (DMI), and high-precision differential GPS measurements. In addition, pavement surface temperature measurements and digital video imaging of the pavement and right-of-way conditions will be included.

This project is a 3-year project that began in September 2008. The first-year efforts are discussed in this report. The project is a joint effort between the Center for Transportation Research (CTR) at The University of Texas (UT) and the Texas Transportation Institute (TTI) at Texas A&M University. Researchers at CTR, working with researchers at the Center for Electromechanics (CEM) at UT, are responsible for developing all aspects dealing with the RDD portion of the TPAD. This work includes developing (1) the TPAD moving platform, (2) the dynamic pavement loading system associated with the RDD, and (3) the dynamic pavement deflection measurement system of the RDD. This effort also includes selecting a manufacturer, interacting with the manufacturer, and then operating the TPAD once it is built. The researchers at TTI are responsible for purchasing essentially all equipment that is not associated with the RDD function, integrating this equipment, with help from CTR and the TPAD manufacturer, into the moving platform, and developing an integrated data acquisition and display system which combines all functions of the TPAD on the same time and distance baselines. Once the TPAD is operational, the TTI researchers will be responsible for operating and managing the integrated data acquisition and display system.

1.2 Outline of Progress during Year 1 Presented in Chapters 2 through 6

Development of the TPAD is being done in several phases, some in parallel, and some sequentially. Critical starting points are the following: (1) select an appropriate moving platform on which to house the dynamic loading and deflection measurement systems associated with the RDD portion of the TPAD, (2) with this platform, evaluate manufacturers' qualifications, (3) select contacting or non-contacting rolling sensors for the RDD function and move forward with developing the hardware and software necessary to permit continuous moving measurements to be performed at speeds in the range of 5 to 10 mph. Significant progress has been made in these areas as discussed in Chapters 2 through 4. A likely moving platform for the TPAD is a modified version of a unique truck-mounted device manufactured by Industrial Vehicles Incorporated (ivi) of Tulsa, Oklahoma. Initial tests with a prototype ivi RDD system are described in Chapter 2. The prototype was developed by ivi at no cost to this project. Initial tests with the prototype ivi RDD were performed at the TxDOT Flight Services Facility at Austin Bergstrom International Airport in July 2009. The tests showed that reasonable dynamic deflection measurements with the prototype are possible with second-generation rolling sensors developed by Lee (2006). With the work presented in Chapters 3 and 4 that is underway to improve the RDD rolling sensors, high-

quality deflection measurements at speeds of 5 mph or more are attainable with contacting sensors. With this information, the CTR and TTI team in concert with the TxDOT Project Monitoring Committee (PMC) decided to use contacting rolling sensors rather than the dramatically more expensive non-contacting sensors that are unproven in this noisy and sometimes dirty environment beneath the TPAD moving platform.

A second important part of the TPAD development is the addition of other survey functions on the moving platform. The TTI research team is responsible for this portion of the project. The additional survey functions include (1) GPR, (2) high-precision differential GPS, (3) surface pavement temperature, and (4) digital video imaging of the pavement and right-of-way conditions. TTI is responsible for selecting and purchasing these systems and then installing them, with help from CTR and the TPAD platform manufacturer. TTI is also responsible for developing the integrated data acquisition and display system. Significant progress has been made on indentifying much of the equipment and developing the first-generation data acquisition and display system. This work is discussed in detail in Chapter 5 and Chapter 6.

To conclude the report, the path forward in Year 2 is briefly discussed Chapter 7.

Chapter 2. Prototype Evaluation Studies at TxDOT Flight Service Facility, ABIA

2.1 Introduction

As discussed in Chapter 1, work on developing the specifications for the TPAD culminated at the end of Year 1 with prototype evaluation studies at the TxDOT Flight Service Facility (simply referred to as FSF) at the Austin Bergstrom International Airport (ABIA). This work was performed as part of Task 1 of Project 0-6005. The studies involved the original UT RDD which was used to perform baseline measurements at 1 mph along a 700-ft section of jointed concrete pavement at the FSF. A potential manufacturer, Industrial Vehicles Incorporated (ivi), also participated. Industrial Vehicles Incorporated is an established manufacturer in the geophysical exploration business and a developer of unique smaller vibroseises. They supplied, at no cost to the project, a prototype RDD that they were developing in-house. With the UT RDD and ivi prototype RDD, evaluation studies described in this chapter were performed. These studies involved continuous and stationary measurements on the jointed concrete pavement at profiling speeds ranging from 1 to 5 mph.

Prior to testing, the deadweight of each RDD was measured with load cells supplied by the Center for Electromechanics (CEM). The static loading measurement system of each device was also evaluated in the field using the CEM load cells. In addition, field calibration of the rolling sensor used with each device was performed at the test site. During testing, continuous profiling with the UT RDD and ivi RDD was conducted with different testing speeds. Finally, stationary deflection measurements at discrete locations across one slab were performed as a means of developing a reference with which to compare the continuous profiles across the slab that were determined with each RDD platform.

2.2 RDD Descriptions

2.2.1 UT RDD

The UT RDD is a truck-mounted device that is used to measure continuous deflection profiles (See Figure 2.1a). The total weight of the UT RDD is about 50 kips. This device is 32 ft in length, 8 ft in width, and approximately 12 ft in height. The UT RDD loading system is shown in Figure 2.1b and is capable of generating static forces of 3 to 40 kips and dynamic sinusoidal forces with peak-to-peak amplitudes of 2 to 70 kips over a frequency range of about 10 to 100 Hz. In typical highway projects, a static hold-down force in the range of 7 to 10 kips and a peak-to-peak dynamic force in the range of 6 to 10 kips at an operating frequency of 30 Hz are used. The combined static and dynamic forces are continuously recorded by four load cells located between the loading rollers and upper loading platform. In normal operations, up to four rolling sensors are used to measure pavement movements (dynamic deflections) under the sinusoidal loading. In this study, only one first-generation rolling sensor was used that was located between the loading rollers (sensor position #1). This sensor is composed a 2-Hz geophone on a 3-wheel cart with 6-in. diameter wheels. The UT RDD with the rolling sensor was used to profile along the pavement at approximately 1 mph (1.6 km/hr). These measurements are considered representative baseline measurements with which all other measurements are compared. In

addition, profiling with the UT RDD was also performed with a second-generation rolling sensor as discussed below.

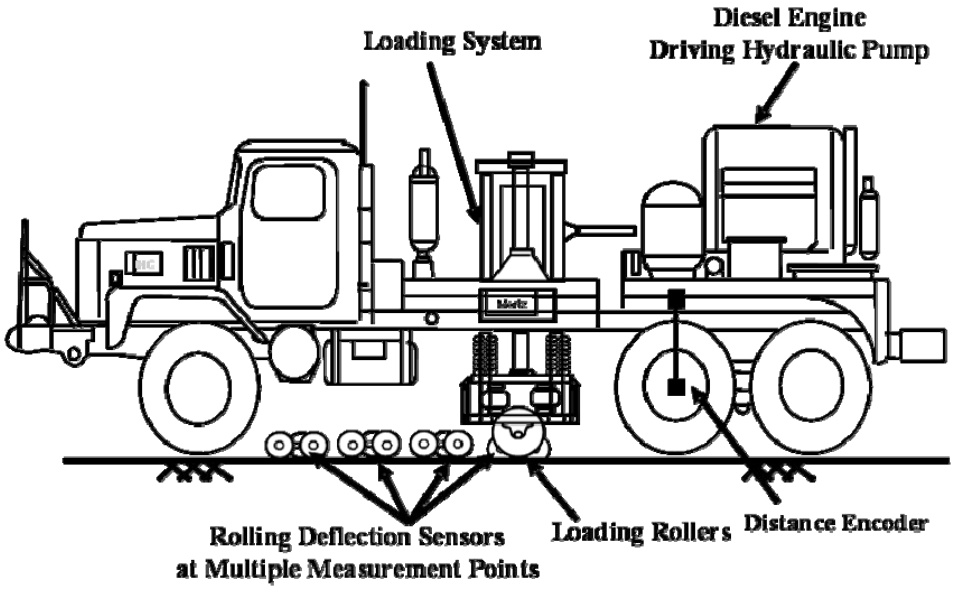

(a)

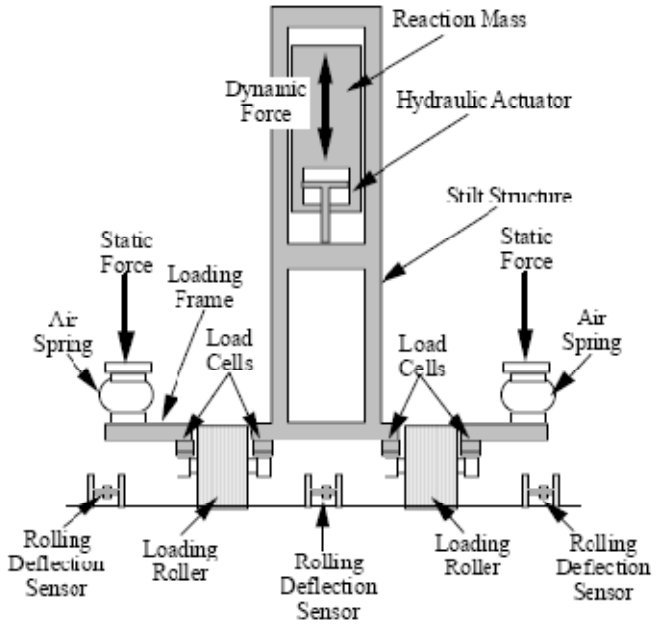

(b)

Figure 2.1: General Arrangement of the UT RDD: (a) Side View of the UT RDD and (b) Cross-Sectional View of the Loading System.

2.2.2 ivi RDD

The prototype ivi RDD is a truck-mounted device (see Figure 2.2a), and its static and dynamic loading mechanism is the same general type as the UT RDD (an electro-hydraulic mechanism). The total weight of the prototype ivi RDD (simply called the ivi RDD hereafter) is about 18 kips. The ivi RDD is 20 ft in length, 7.5 ft in width, and 7.8 ft in height. The loading system, shown in Figure 2b, is able to generate static forces of 3.4 to 14 kips and dynamic sinusoidal forces with a peak-to-peak amplitude of 2 to 24 kips over a frequency range of about 7 to 200 Hz. This machine has a speed control system in the range of 1 to 10 mph (Christensen, 2009).

(a) TPAD Moving Platform

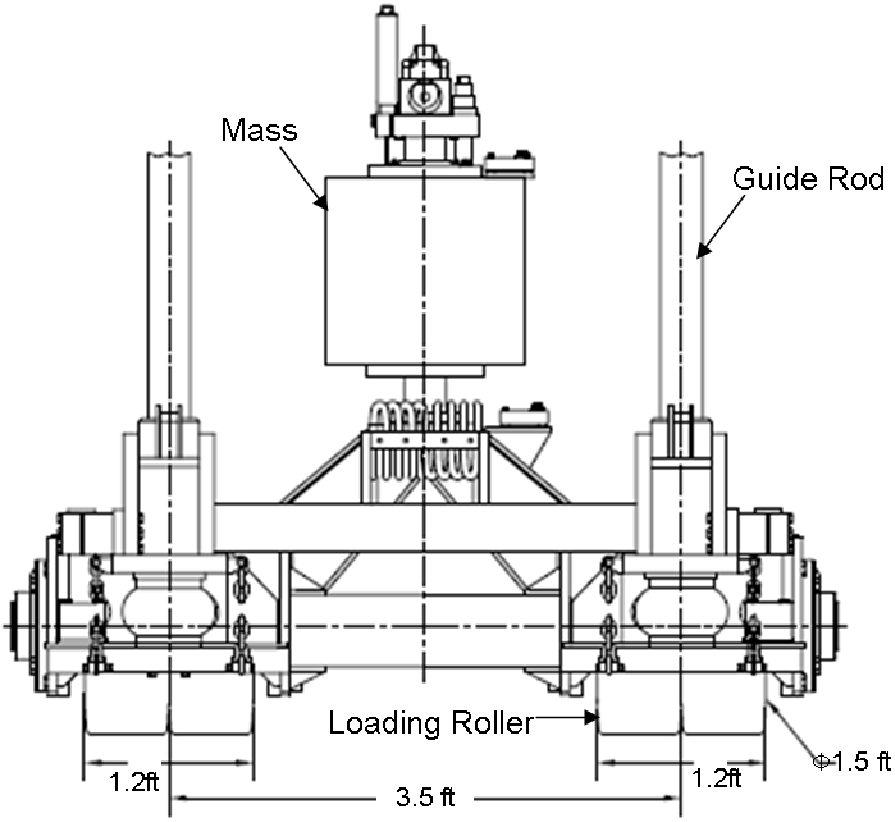

(b) Prototype ivi RDD Loading System

Figure 2.2: Prototype ivi RDD (Potential Configuration of TPAD): (a) Photograph of Prototype ivi RDD (b) Cross-Sectional View of Prototype ivi RDD Loading System (Christensen, 2009).

2.3 Description of Testing Site

Testing with the UT RDD and ivi RDD was performed at the TxDOT Flight Service Facility (FSF). The pavement at this facility is a jointed-concrete pavement (JCP) that has three different slab thicknesses and several transition zones. RDD profiling was performed along several testing paths. However, the results presented here are along Path E which is shown in Figure 2.3. In the east-west direction, Path E consists of the following: (1) a 200-ft long section with 16-in. thick slabs and (2) the remaining 500-ft is composed of 8-in. and 10-in. slabs. The 16-in. thick slabs are 25 ft in length and 25 ft in width while the 8-in. and 10-in. thick slabs are 12.5 ft in length and 12.5 ft in width. The testing paths are named by a letter (for north-south testing paths) and by a number (for east-west testing paths) on the drawing of the facility. Path E, shown in Figure 2.3, crosses all three types of slabs.

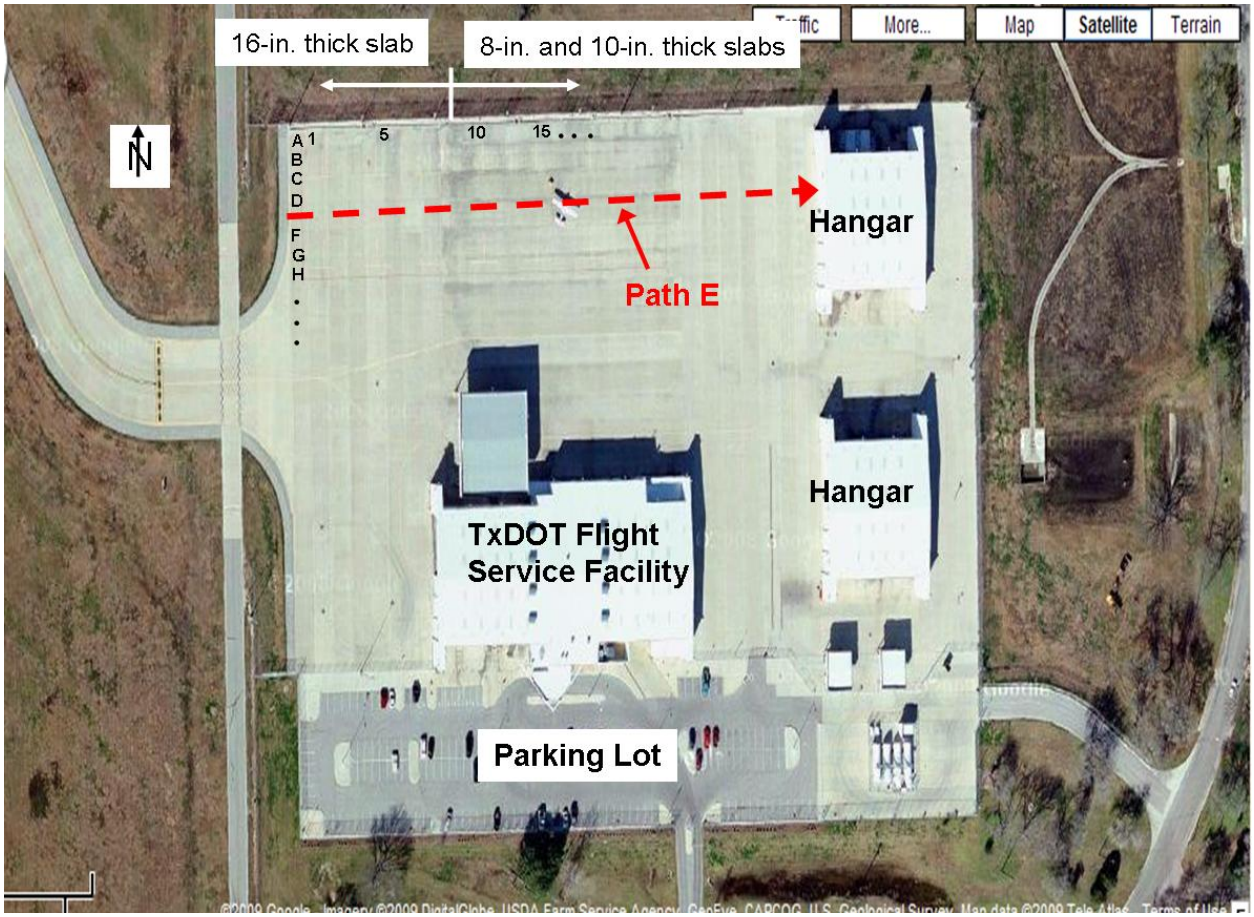

Figure 2.3: Layout of Testing Location, TxDOT Flight Service Facility (FSF)

2.4 Weight Measurement

The deadweights of the UT RDD and ivi RDD were measured using static load cells supplied by the Center for Electromechanics (CEM). The CEM load cells were placed beneath the vehicle's contact points which are the front wheels, loading rollers, and rear wheels. The UT RDD was weighed with the rollers in the up and down positions while the ivi RDD was only

weighed with the rollers in the up position. The static loads applied by the UT RDD and ivi RDD are shown in Figure 2.4.

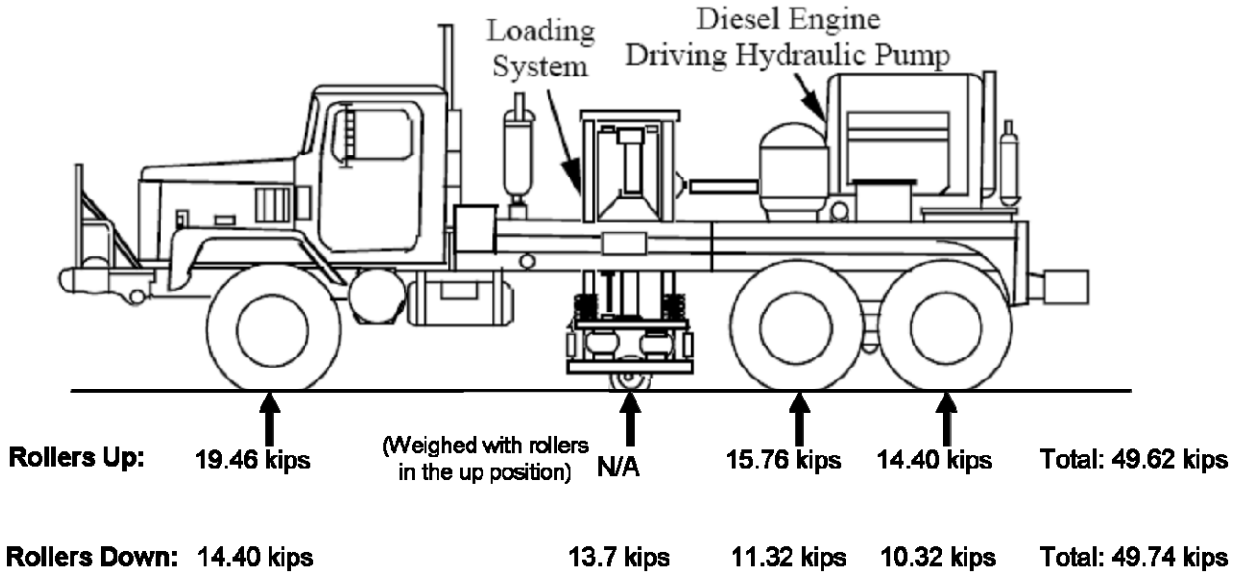

(a)

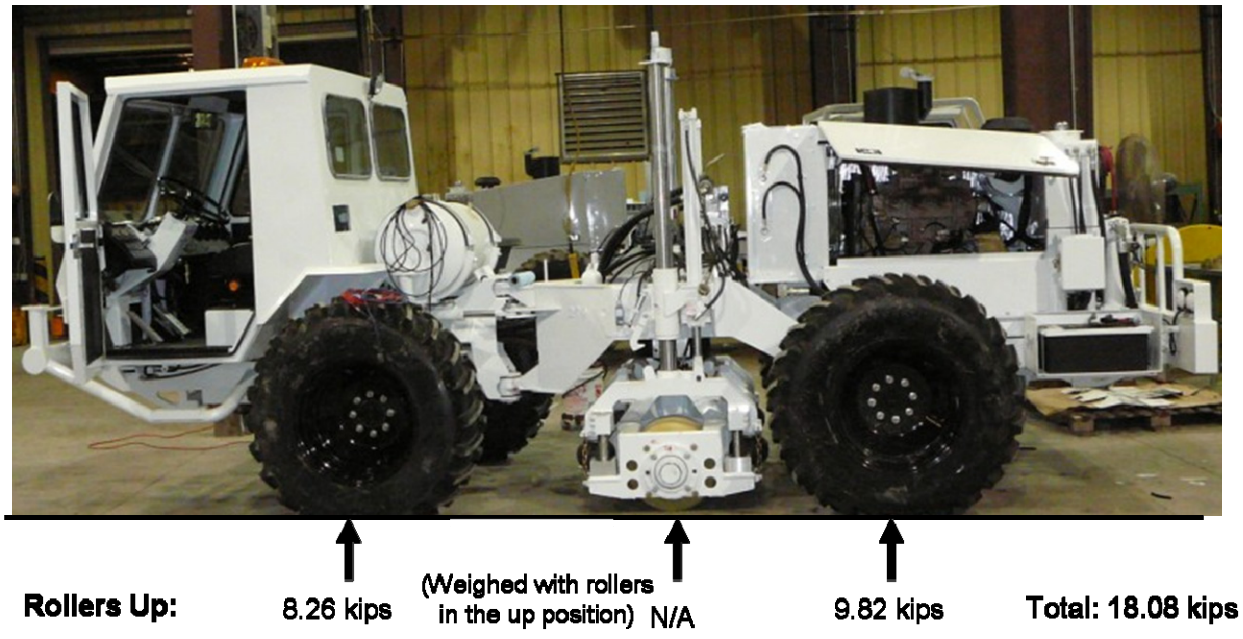

(b)

Figure 2.4: Static Loads Applied by RDD: (a) UT RDD and (b) ivi RDD

2.5 Calibration of Static Loading

Static load calibrations of the UT RDD and ivi RDD were conducted prior to testing. The UT RDD has four load cells to measure static and dynamic forces applied to the pavement. The four load cells are located between the loading rollers and the upper loading platform. On the other hand, the ivi RDD has pressure transducers to measure static forces and accelerometers (one on the base plate and the other on the hydraulic mass) to measure dynamic forces. At the time of the load calibration, no dynamic load cells were available. Thus, only static load calibrations of the UT RDD's are presented. The dynamic load calibrations will be conducted in the future.

For the UT RDD, the CEM load cells were placed beneath the loading rollers. As the static forces were incrementally increased, readings from the RDD load cells and the CEM load cells were recorded and compared. The same testing procedure was applied to the load calibration of the ivi RDD. The load calibration curves of both devices are shown in Figures 2.5a and 2.5b, respectively. The measured calibration curves show that the UT RDD exhibits an accurate force measurement up to 5,000 lbs and then began to overestimate the actual force, with an overestimation of about 7% at 14,000 lb. In pavement testing with the UT RDD, the hold-down force is often around 10,000 lb. In this case, there is an overestimation in the static load of about 7%, which has essentially no impact on the dynamic deflections created during RDD testing.

As shown in Figure 2.5b, the ivi RDD showed a poor static force measurement. With the static force of 10,000 lbs, the ivi RDD generated an overestimation of about 22% which will need to be corrected by the manufacturer if this device is selected for purchase. However, ivi personnel did acknowledge that they had spent little time on this part of the device so that the demonstration could be performed on time. Ivi plans to improve the load measurement system.

2.6 Description of Rolling Sensors

The second-generation rolling sensor (only Sensor #1) was used for testing with the UT RDD and ivi RDD. The second-generation rolling sensor consists of three rolling wheels (9 in. diameter) and positions a 2-Hz geophone at the geometric center of the three-wheel cart. Each wheel is coated with a 60-D polyurethane (golf-ball coating stiffness) tread with a 0.25-in. thickness. During testing, the hold-down force of 3 psi was applied at higher testing speeds. Figure 2.6a shows a photograph of the second-generation rolling sensor and its position between the two loading rollers. More details on the second-generation rolling sensor for the UT RDD are presented in Lee's dissertation (Lee, 2006).

On the other hand, the ivi RDD was equipped with a modified second-generation rolling sensor that was originally built by CTR. This modification was due to different size and design of the ivi RDD loading frame. Figure 2.6b shows a diagram of the ivi RDD sensor and the sensor position relative to the loading rollers and loading frame.

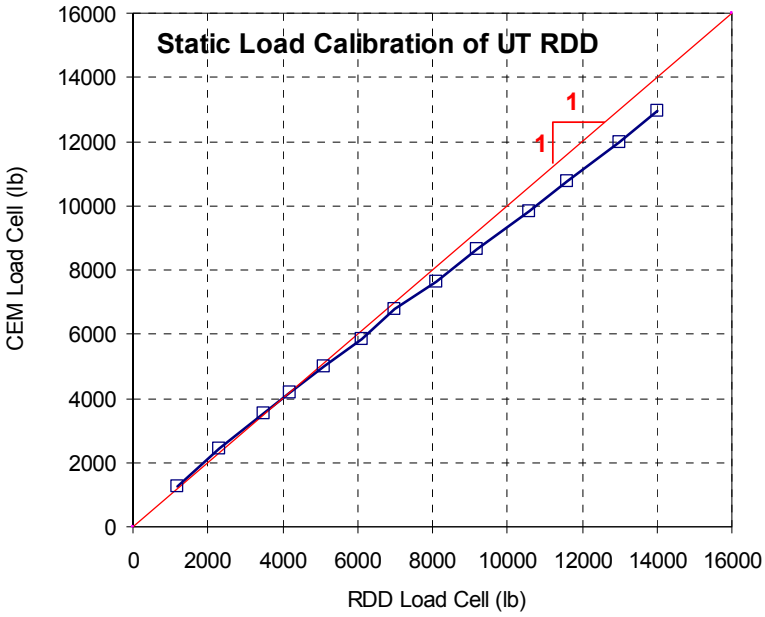

(a)

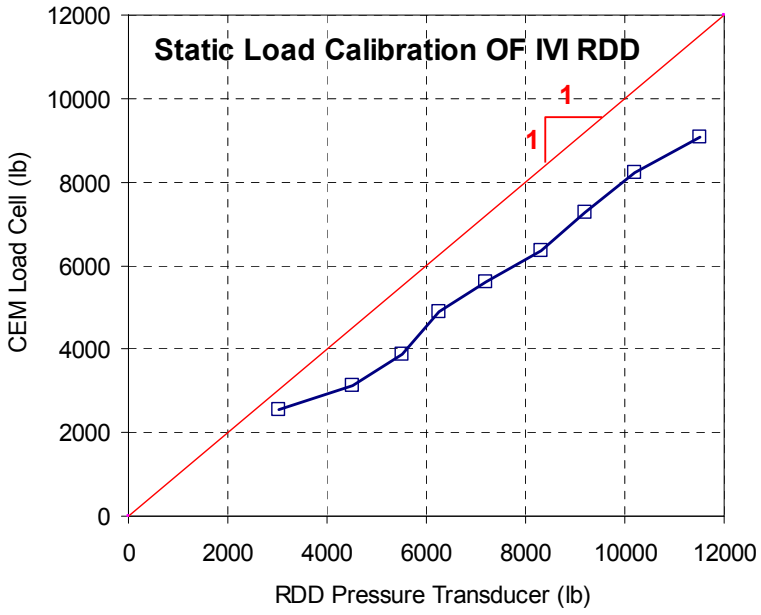

(b)

Figure 2.5: Calibration of Static Loading Applied by Rollers: (a) UT RDD and (b) ivi RDD

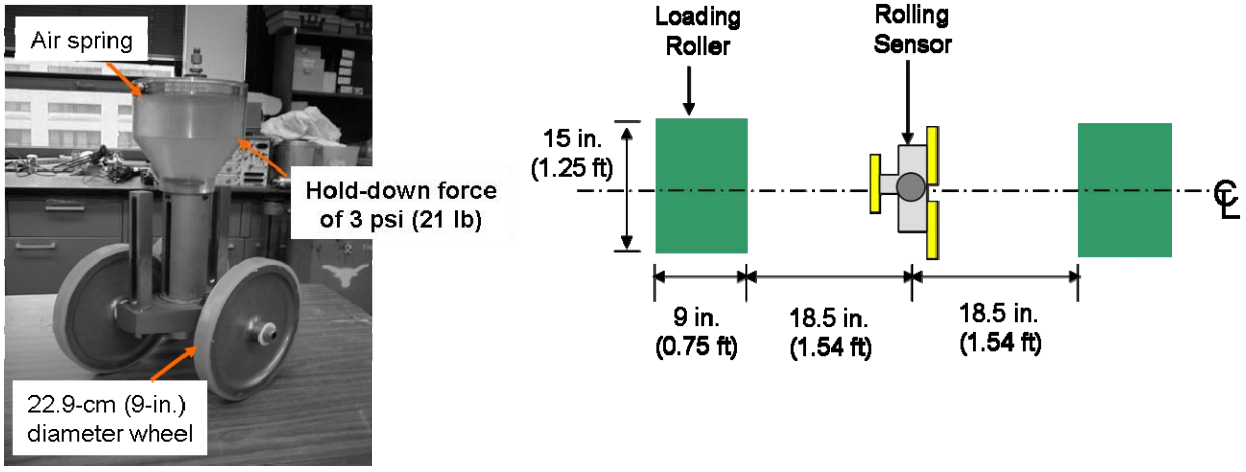

(a)

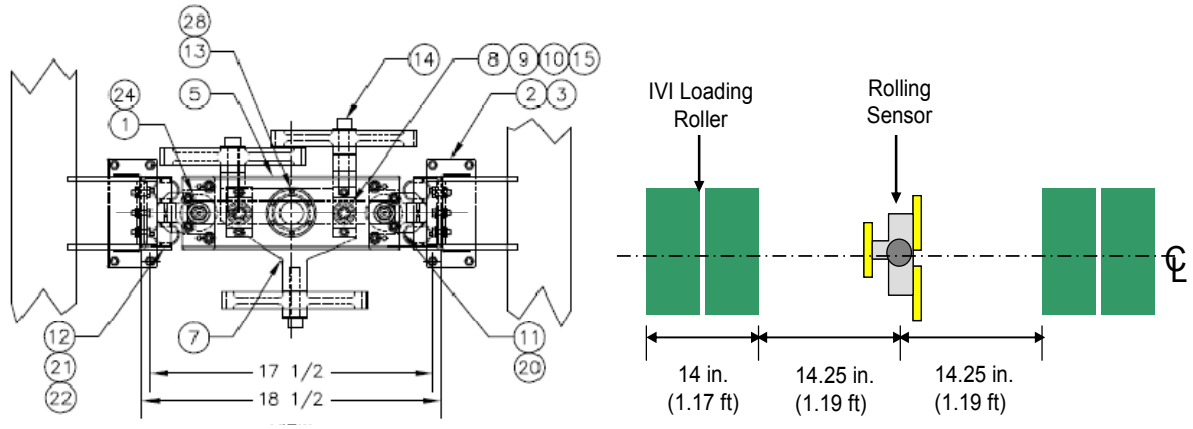

(b)

Figure 2.6: Rolling Sensors and Sensor Position Relative to the Loading Rollers during Testing: (a) UT RDD and (b) ivi RDD

2.7 Field Sensor Calibration

Field sensor calibrations of the UT RDD and ivi RDD rolling sensors were conducted prior to testing. This practice ensures that each rolling sensor is performing properly at each testing site. The field calibration involves fixing a small metal plate to the pavement surface using "fast-set" epoxy. Once the metal plate is glued to the pavement, a calibrated reference transducer is screwed to this plate. A high-precision accelerometer (Wilcoxon 736T) was selected as the transducer to measure the dynamic motion on the pavement surface. Each RDD was then used to perform swept sine loading over a range of frequencies from 20 to 60 Hz. The results of the field sensor calibrations are shown in Figures 2.7.

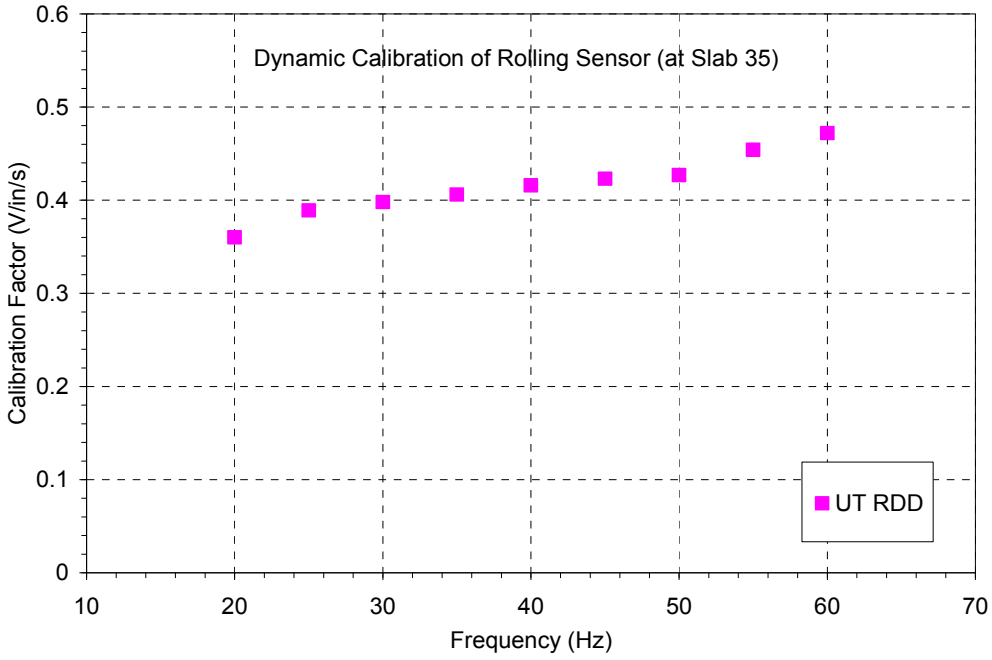

(a)

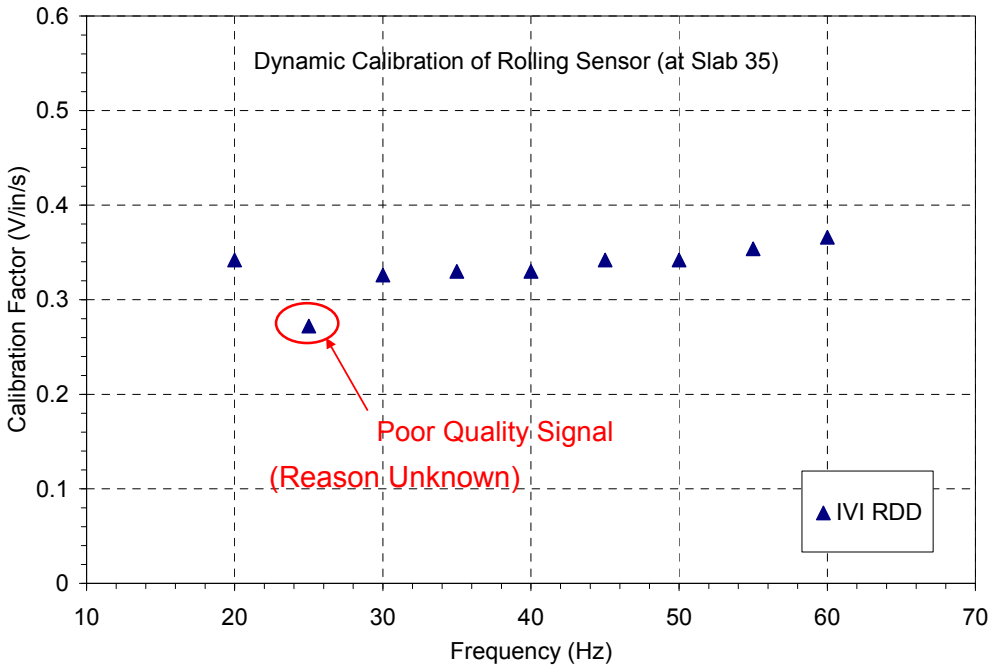

(b)

Figure 2.7: Dynamic Calibration of the Rolling Sensors at the TxDOT Flight Service Facility (FSF): (a) UT RDD and (b) ivi RDD

2.8 Deflection Measurements

2.8.1 Preliminary Study at the FSF Pavement Using the UT RDD and First-Generation Rolling Sensors

Several different test paths were profiled with the UT RDD to select an optimum testbed. Two longitudinal paths (Paths E and Q) and four cross paths (Cross Paths 1, 35, 45, and 63) were profiled (see Figure 2.3 for general locations). Only deflection data for profiling along Path E are presented in this report. Path E was selected because it is away from the normal traffic pattern at the TxDOT Flight Service Facility and it also has a range of slab thicknesses. Path E shows a clear pattern of joints and mid-slab areas, with slab thicknesses and joint types varying along the testing path as shown by the relative changes in deflections along the profile. In addition, the data is part of an initial longer-term study of temperature effects on the RDD deflection measurements. The RDD was used to profile Path E at different surface pavement temperatures, ranging from 91°F to 128°F. The deflection profiles along Path E at these temperatures are shown in Figure 2.8. As the temperature increases, the deflections at joints dramatically drop while the deflections in the mid-slab areas increase slightly. This observation can be explained by the combination of slab curling and slab expansion with increasing pavement temperature.

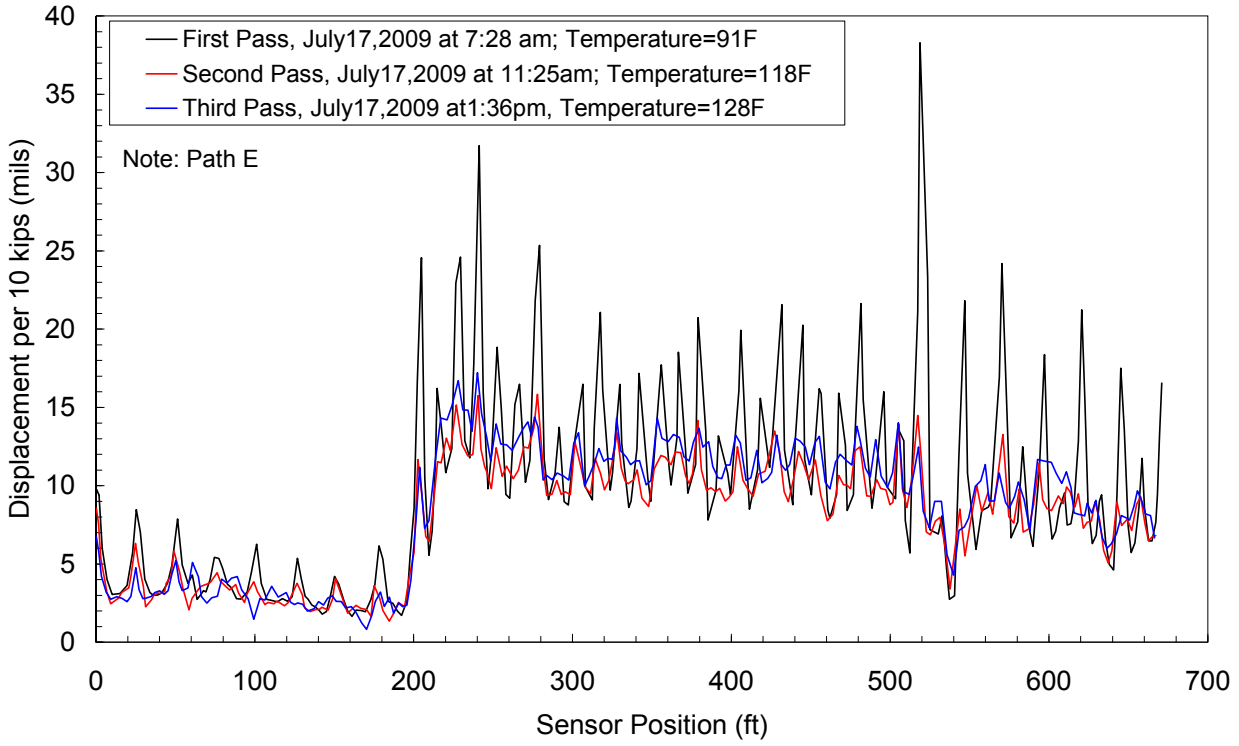

Figure 2.8: Continuous Deflection Profiles Measured by the UT RDD with First-Generation (6-in.-diameter wheels) Rolling Sensors along Path E for Different Pavement Surface Temperatures

2.8.2 Continuous Profiling with the UT RDD

Based on the preliminary study, temperature is a major factor affecting slab behavior and must be considered in all future tests. To minimize the impact of temperature on the deflections of the concrete slabs (from warping, curling, expansion, and shrinkage), testing with the UT RDD and ivi RDD was performed between 6:00 a.m. and 11:00 a.m. when the pavement surface temperature was less than about 100°F. The UT RDD was also used to profile Path E several times with testing speeds of 1, 2, 3, and 4 mph. To profile at higher rolling speeds without sacrificing data accuracy, the rate of sampling the rolling sensor output was increased from 256 Hz to 512 Hz at 1 mph. During testing at other speeds, the sampling rate was proportionately increased as the rolling speed increased.

Current RDD signal processing is a time-based method that averages deflection data over a given time, with the time called the "averaging" time and denoted as "t90" in the following figures. The UT RDD was used to first profile Path E at 1 mph with a sampling rate of 512 Hz. In signal processing, two different t90s of 1 and 2 sec were used to investigate the effect of t90 on the deflection profiles. As shown in Figure 2.9, using t90 of 2 seconds generates slightly lower deflections at joints but almost the same level of deflections at the mid-slab areas. This observation is more clearly seen in the 8-in. and 10-in. thick slabs rather than 16-in. thick slabs. The deflection profile at 1 mph with t90 of 1 sec is hereafter used as a reference to show the structural conditions along Path E.

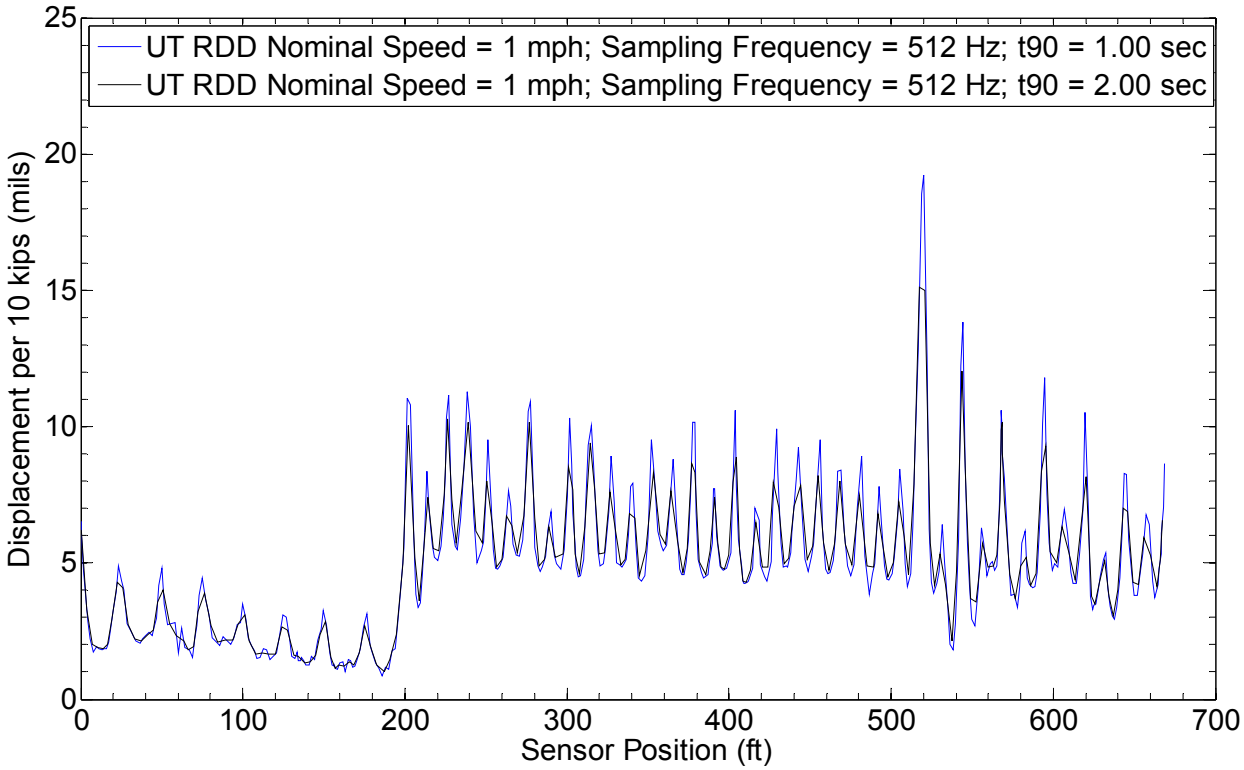

Figure 2.9: UT RDD Deflection Profiles with Testing Speed of 1 mph; Comparison of "Averaging" Times (t90)

Deflection profiles with testing speeds of 2, 3, and 4 mph are compared with the deflection profile determined at 1 mph in Figures 2.10, 2.11, and 2.12, respectively. In data processing, as the testing speed was increased, t90 was proportionately decreased to obtain same distance resolution in the data. The deflection profiles evaluated at 1 and 2 mph show very similar results (Figure 2.10). The testing speed of 3 mph caused more noise in the signals, but the results are in reasonable agreement with the deflection profile at 1 mph (Figure 2.11). The deflection profile determined with a testing speed of 4 mph shows more noise (Figure 2.12). However, a reasonable comparison between the deflection profiles determined at 1 mph still exists.

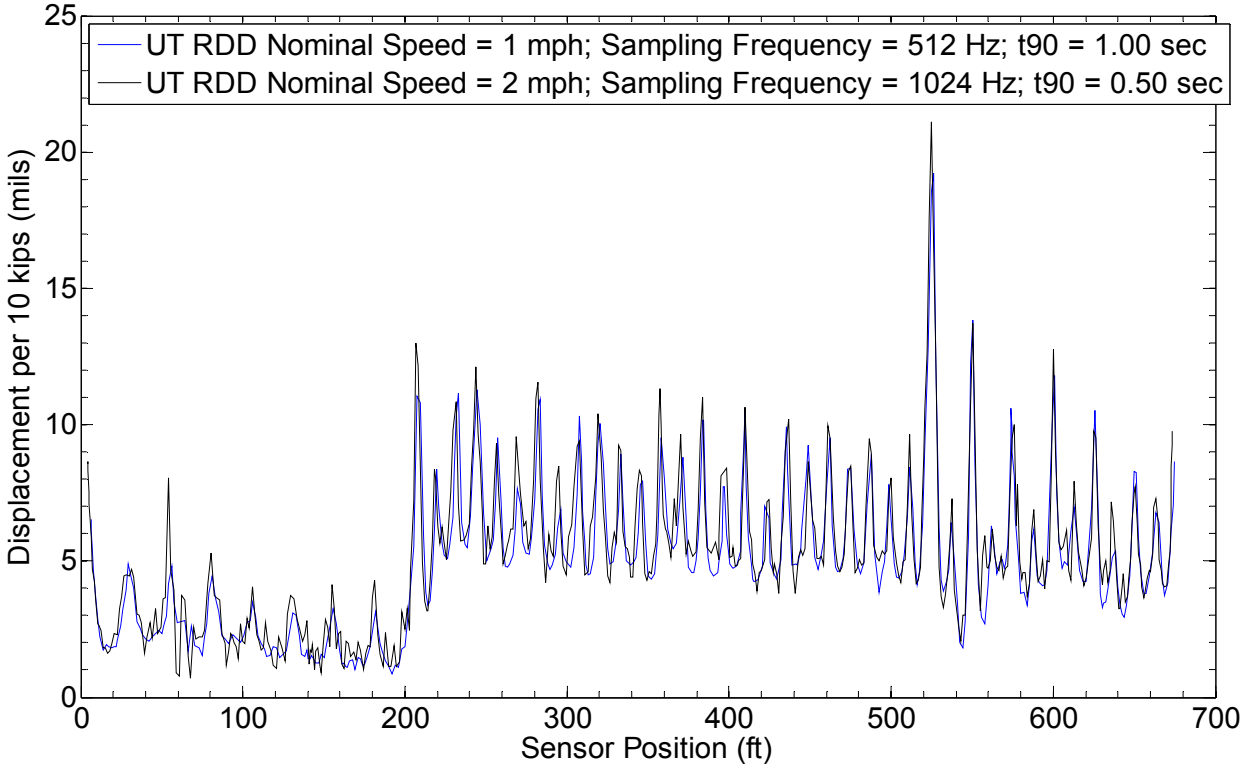

Figure 2.10: UT RDD Deflection Profiles with Testing Speeds of 1 and 2 mph.

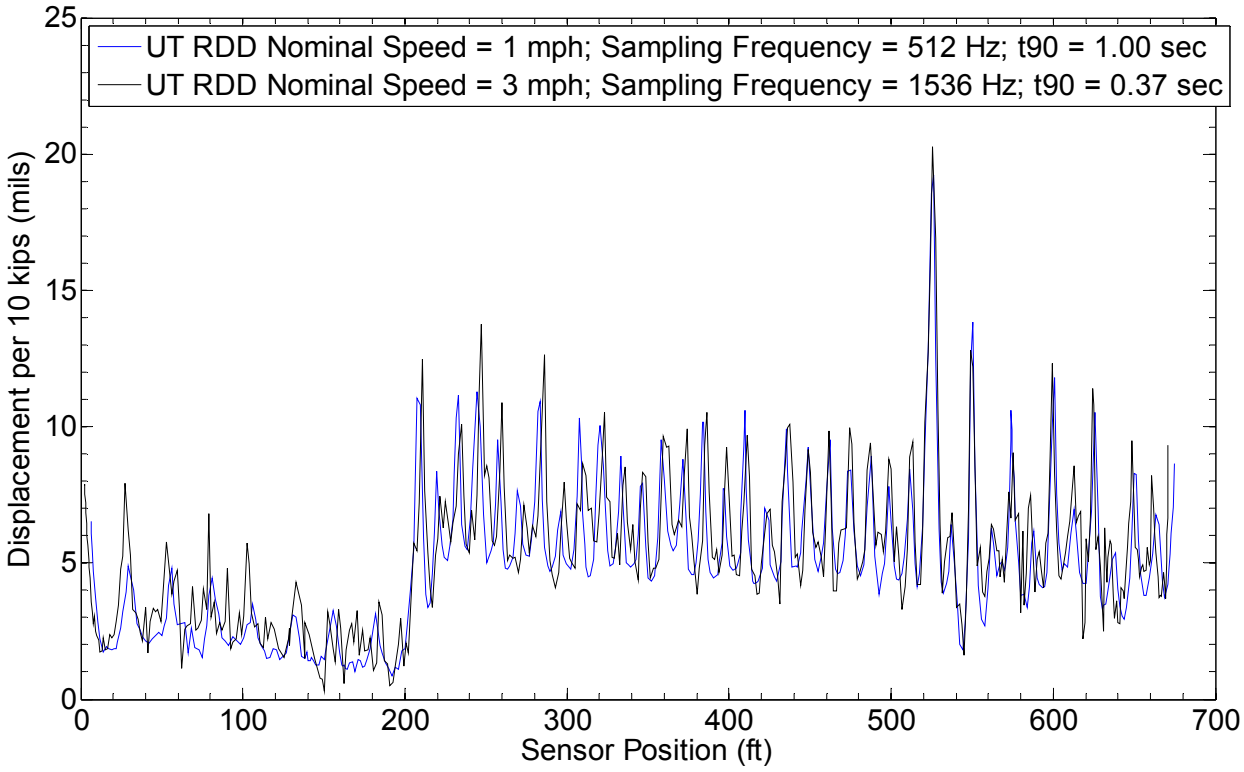

Figure 2.11: UT RDD Deflection Profiles with Testing Speeds of 1 and 3 mph.

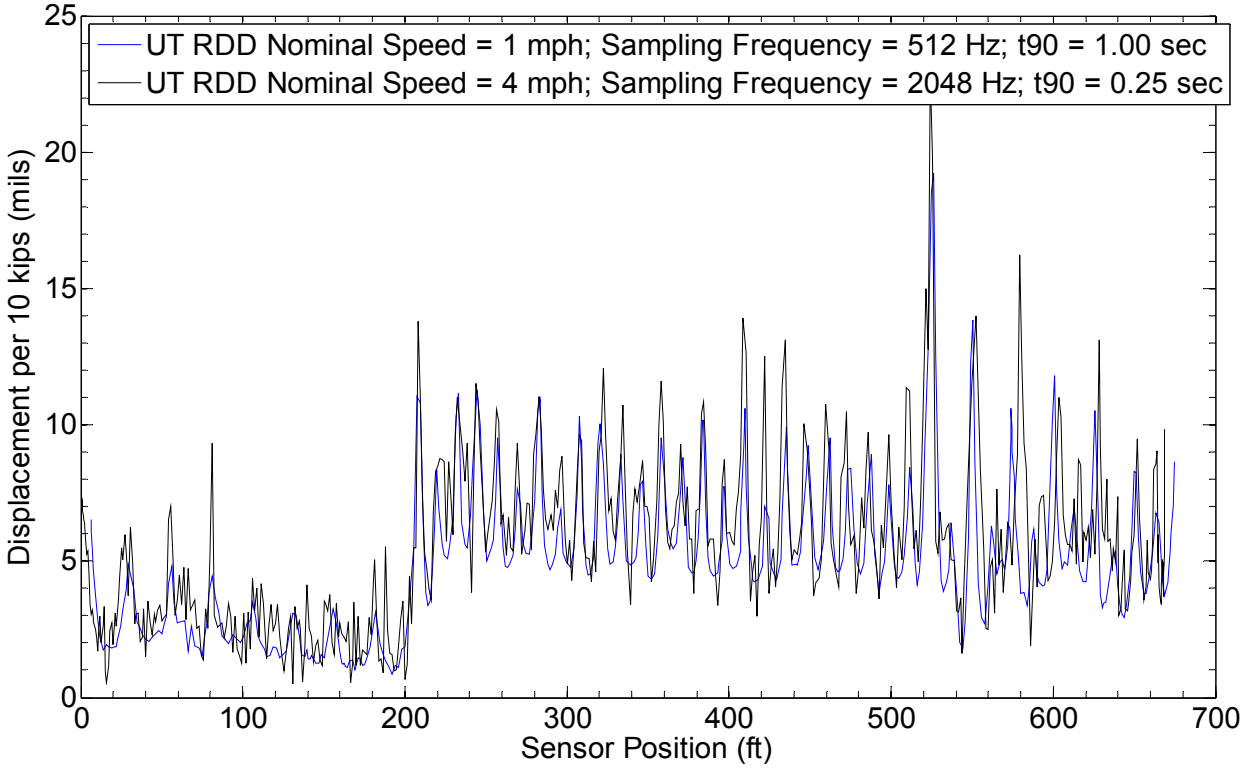

Figure 2.12: UT RDD Deflection Profiles with Testing Speeds of 1 and 4 mph.

2.8.3 Stationary Deflection Measurements with the UT RDD

Stationary deflection measurements with the UT RDD were performed at seven discrete locations on one slab so that the responses of the slab and adjacent joints in the stationary mode could be compared with the same measurements performed while moving. In the stationary tests, noise due to the sensor rolling is not involved and also the "averaging" technique is not used in the signal processing when the sensor is stationary. In other words, each stationary deflection measurement generates a point deflection not an averaged deflection over a pre-determined distance. The results presented here are for Slab 43 (an 8-in. thick slab). The comparison of continuous profiling and stationary deflection measurements is shown in Figure 2.13. Generally, continuous profiling at the testing speeds of 1 and 2 mph show good agreement with the stationary deflection measurements. The continuous profiling generates essentially the same level of mid-slab deflections as the stationary measurements. However, the stationary measurements at the joints exhibit slightly higher deflections. This relative comparison was expected because the rolling measurement averages the deflection over some distance, not a single point as done in each stationary test.

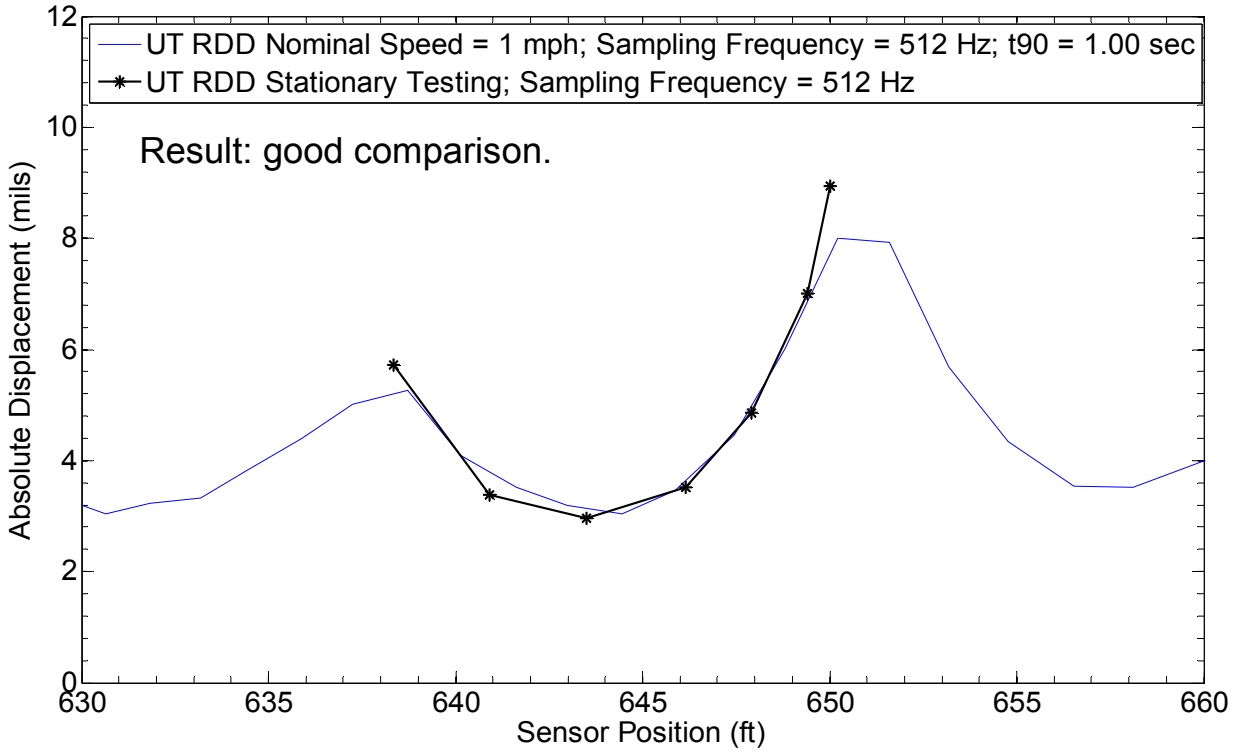

(a)

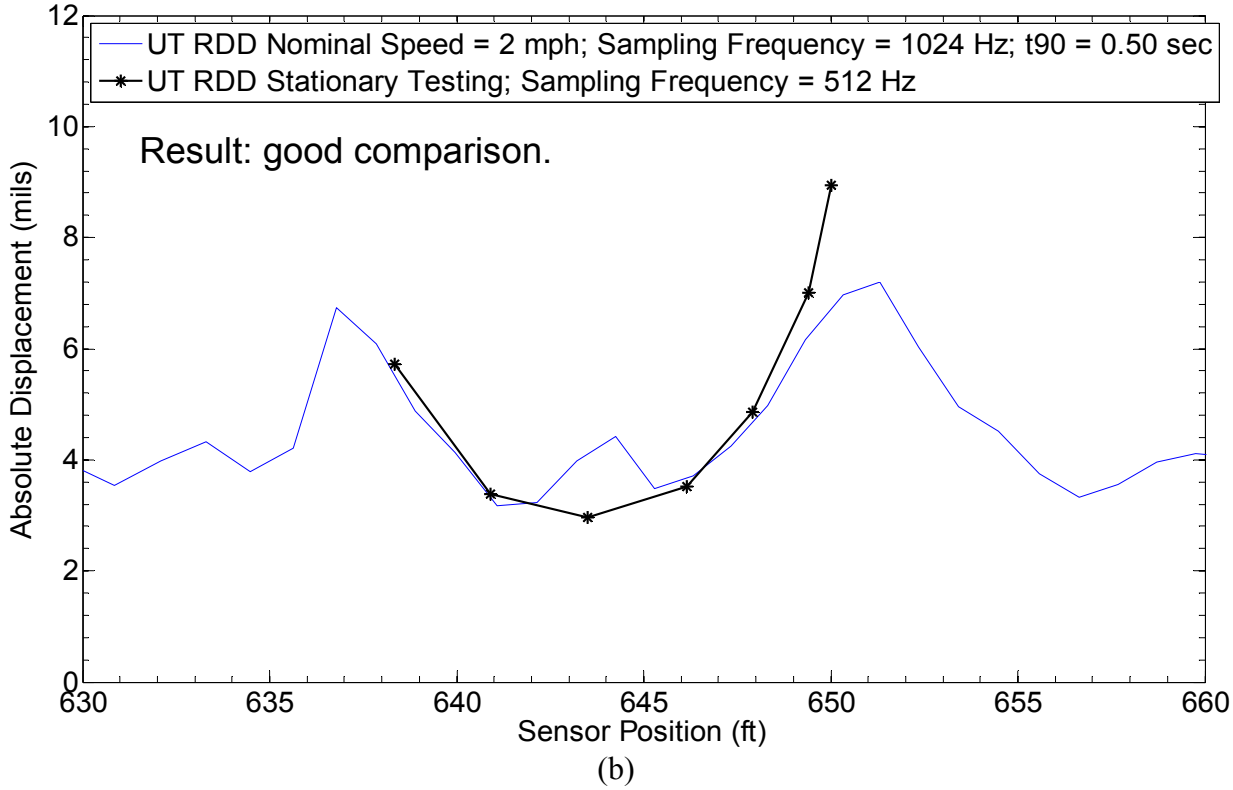

(b)

Figure 2.13: UT RDD Deflection Measurement on Slab 43 (8-in. Slab): (a) Stationary and Testing Speed of 1 mph and (b) Stationary and Testing Speed of 2 mph.

2.8.4 Continuous Profiling with the ivi RDD

Continuous profiling with the ivi RDD was also conducted in the morning between 6:00 a.m. and 11:00 a.m. in order to minimize the temperature effect. The ivi RDD was used to profile the same path (Path E) several times with testing speeds of 1, 2, 3, 4, and 5 mph. A sampling rate of 512 Hz was used for the 1-mph testing speed was done with the UT RDD. As the rolling speed was increased, the sampling rate was proportionately increased. In data processing, t90 was proportionately decreased with increasing testing speeds. The ivi RDD has two accelerometers to estimate dynamic forces applied to the pavement: one on the base plate and the other on the mass. The dynamic load level was, however, uncertain at the time of testing because the dynamic force measurement could not be calibrated due to the absence of load cells capable of measuring dynamic loads. Assuming the weight of the hydraulic mass and base plate, the dynamic forces with different testing speeds were approximated using the accelerometer readings. These results are shown in Figure 2.14. It seems that the level of the dynamic force was considerably higher than the force applied by the UT RDD to the pavement.

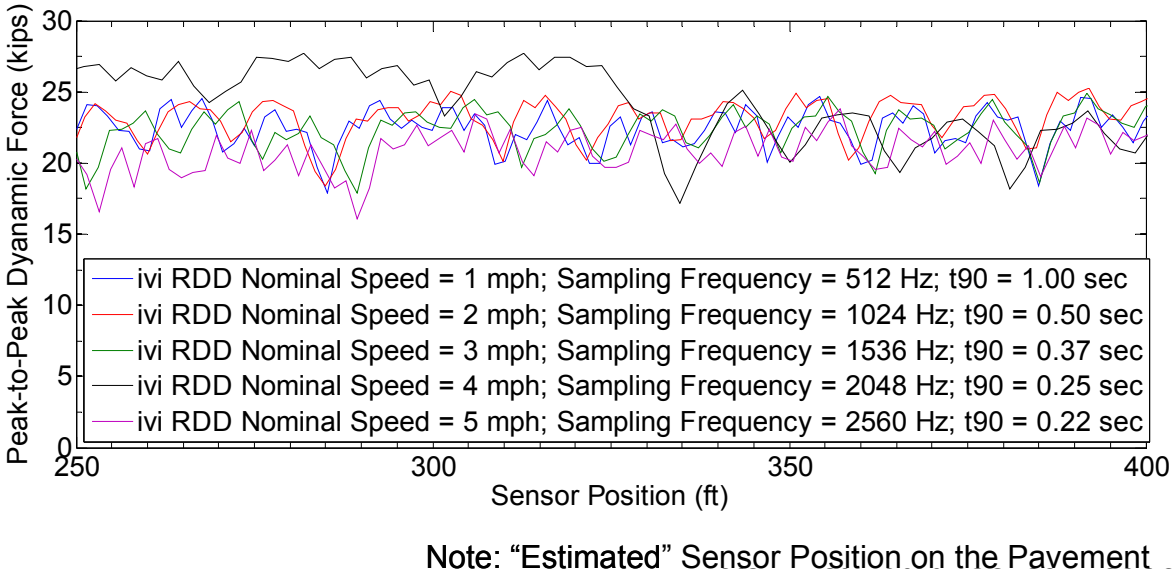

Figure 2.14: ivi RDD Comparison: Peak-to-Peak Dynamic Force with Different Speeds of 1, 2, 3, 4, and 5 mph on an 8-in. thick slab

Because slower testing speeds generate lower noise due to rolling, the deflection profile determined with the ivi RDD moving at 1 mph with t90 of 1 sec is used as the reference profile. The deflection profiles with ivi RDD testing speeds of 1 and 2 mph are shown in Figure 2.15a and 2.15b, respectively. The deflection profile with 1 mph shows the same pattern as the UT RDD. The ivi RDD profiling at 2 mph generates the same profile as testing at 1 mph. The comparison of 1 and 2 mph, shown in Figure 2.16, is an expanded section between Stations 25+0 and 40+0. The comparison of the profiles determined at 1 and 3 mph between Stations 30+0 and 45+0 is shown in Figure 2.17. The deflection profiles determined with testing speeds of 4 and 5 mph are shown in Figures 2.18 and 2.19, respectively.

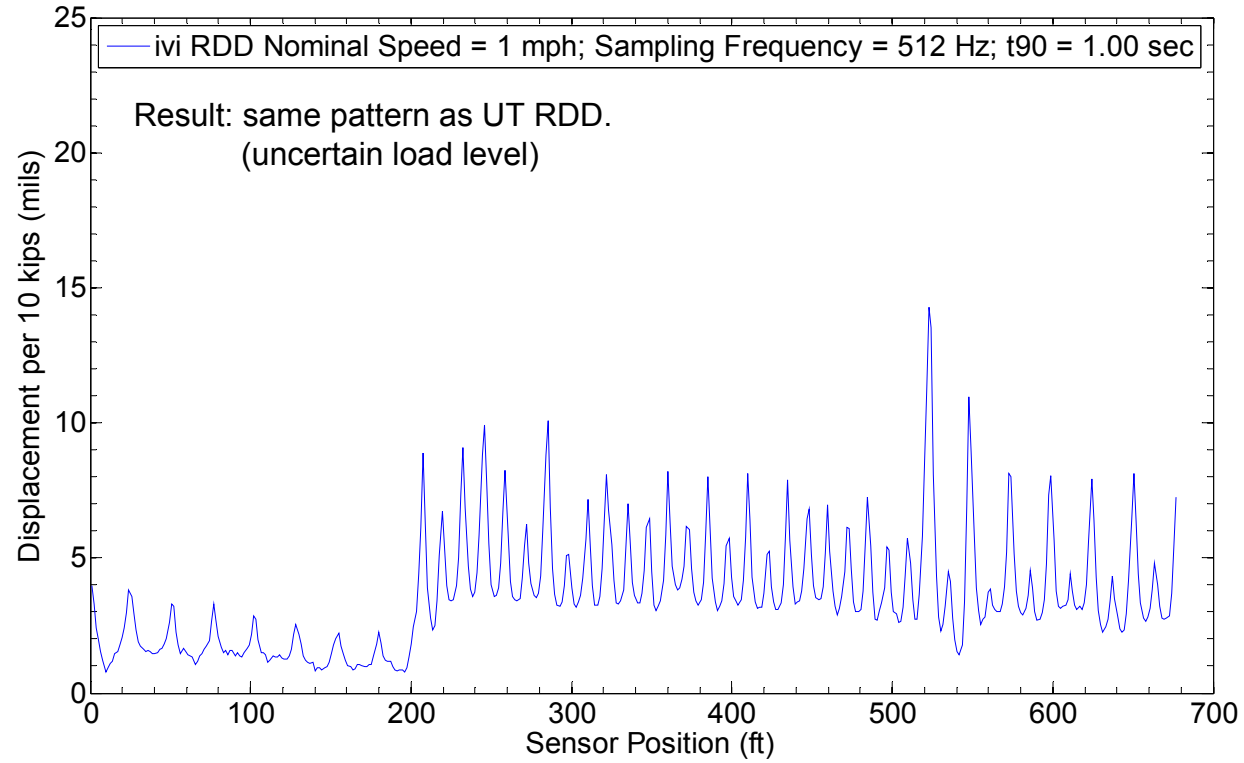

(a)

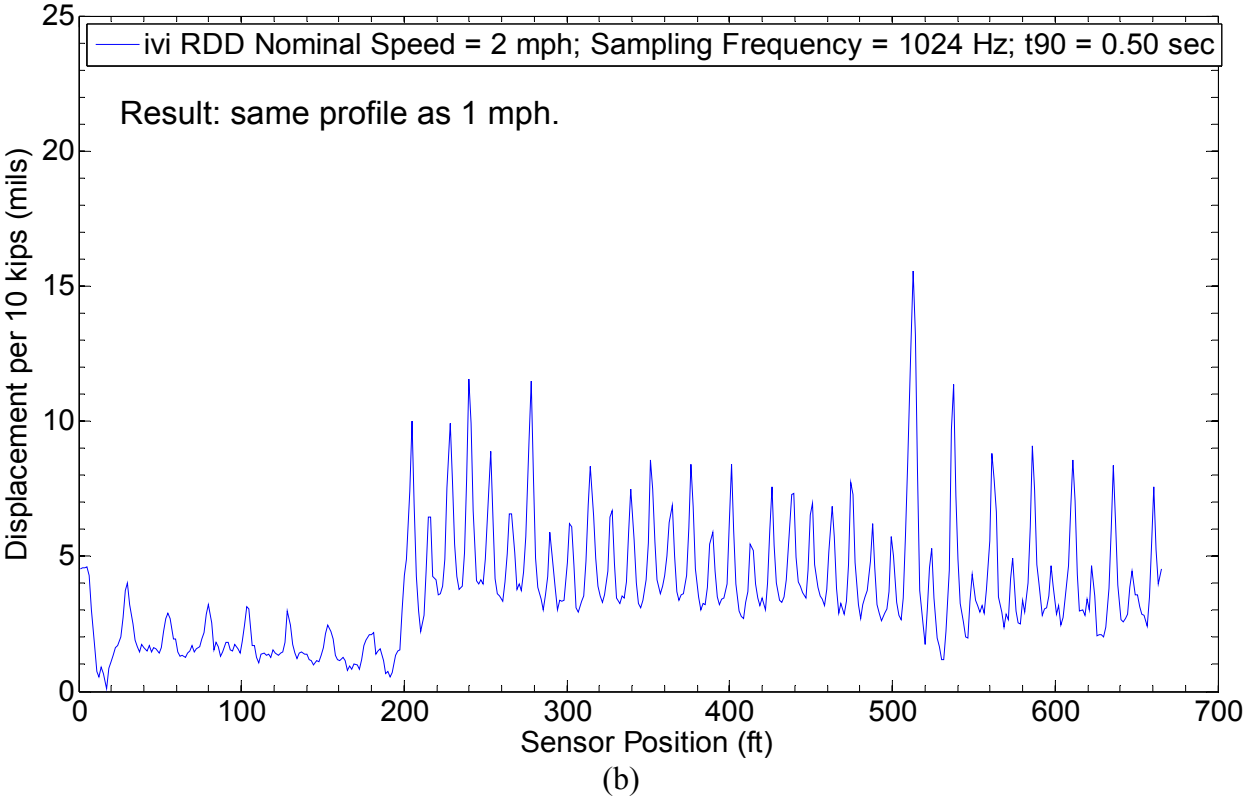

(b)

Figure 2.15: ivi RDD Deflection Profile with Testing Speed of: (a) 1 mph and (b) 2 mph

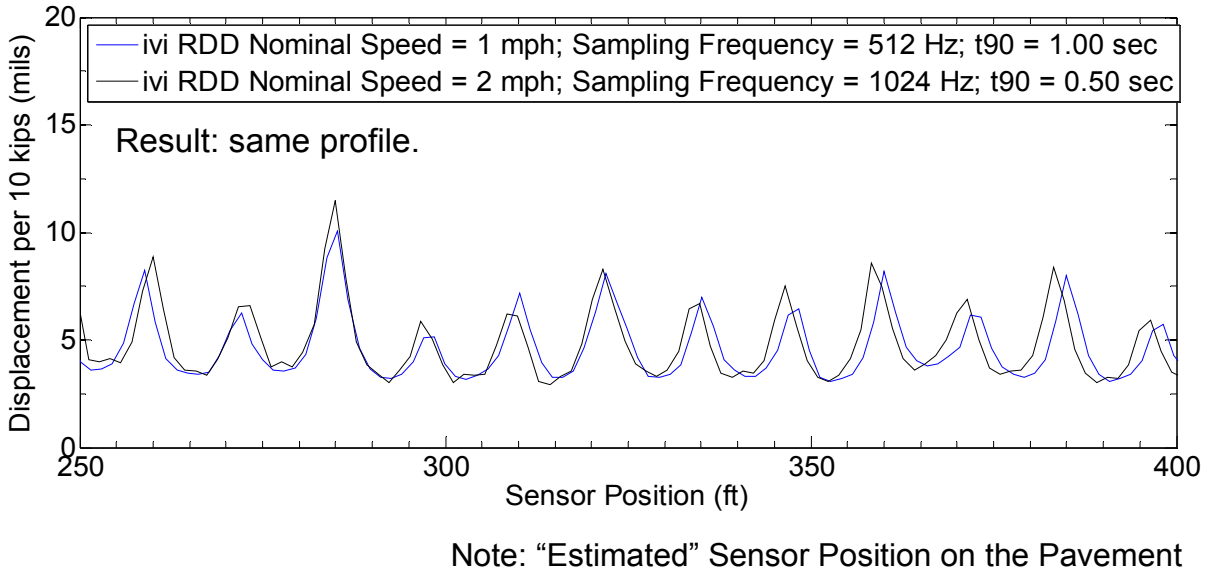

Figure 2.16: ivi RDD Comparison: Testing Speeds of 1 and 2 mph on 8-in. Slabs.

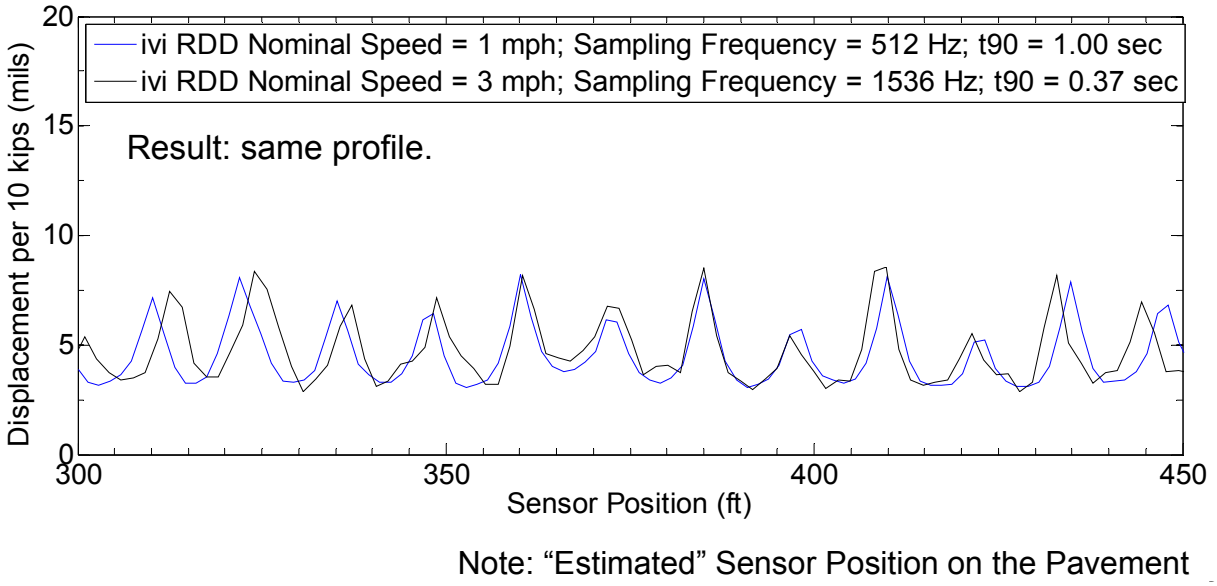

Figure 2.17: ivi RDD Comparison: Testing Speeds of 1 and 3 mph on 8-in. Slabs.

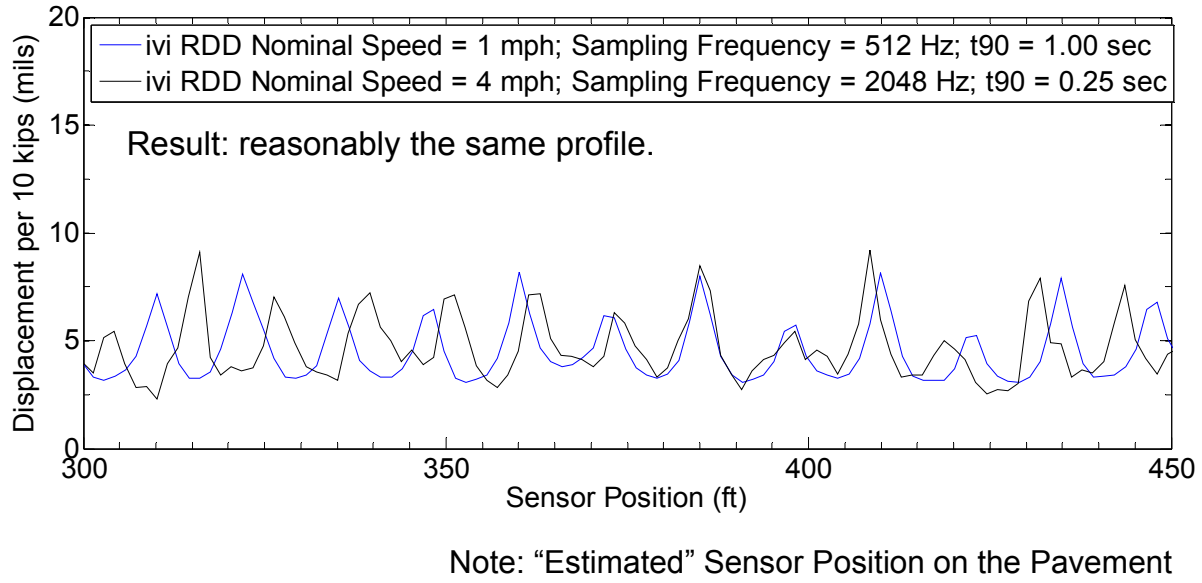

Figure 2.18: ivi RDD Comparison: Testing Speeds of 1 and 4 mph on 8-in. Slabs.

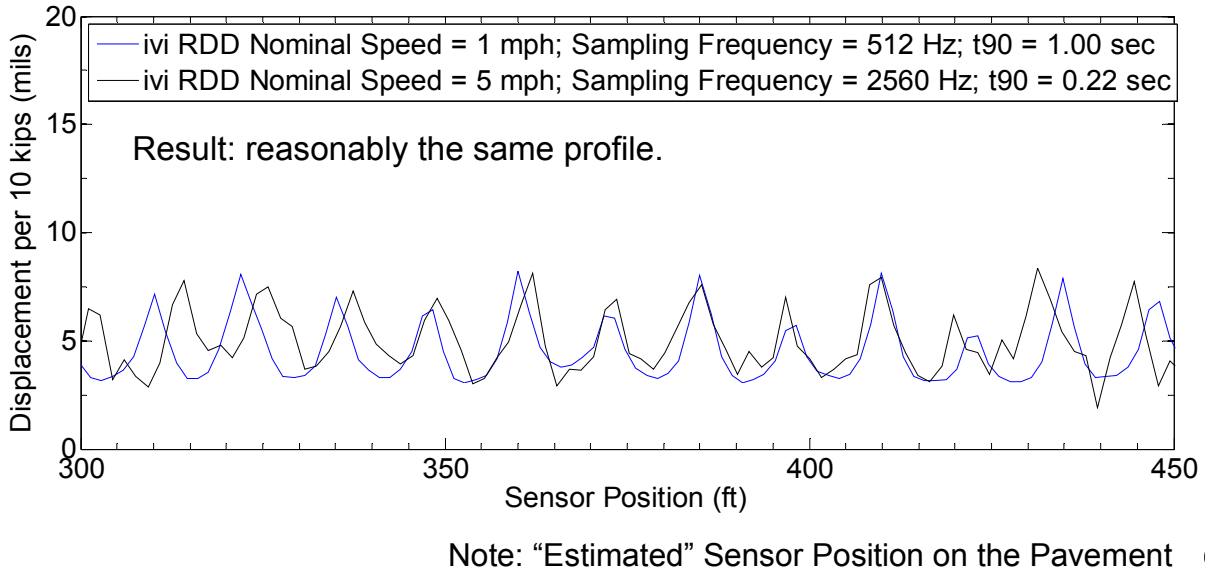

Figure 2.19: ivi RDD Comparison: Testing Speeds of 1 and 5 mph on 8-in. Slabs.

(Note: Peaks at different speeds are not coincident because of the lack of resolution in the distance measurements in the prototype demonstration.)

2.8.5 Stationary Deflection Measurements with the ivi RDD

Stationary deflection measurements with the ivi RDD were performed on the same slab as the UT RDD tests, Slab 43 (8-in. thick slab). During testing, five discrete locations were selected along the slab. The comparison of continuous and stationary deflection measurements is shown in Figure 2.20. One data point, the fourth location of the stationary deflection measurements, was missed because of inappropriate sensor readings (distorted signal readings for unknown reasons). In general, the continuous profiling at testing speeds of 1 and 2 mph shows good agreement with the stationary deflection measurements. The stationary profiling has almost the same deflection level in the mid-slab area but higher deflections at the joints compared to the continuous deflection measurements as expected.

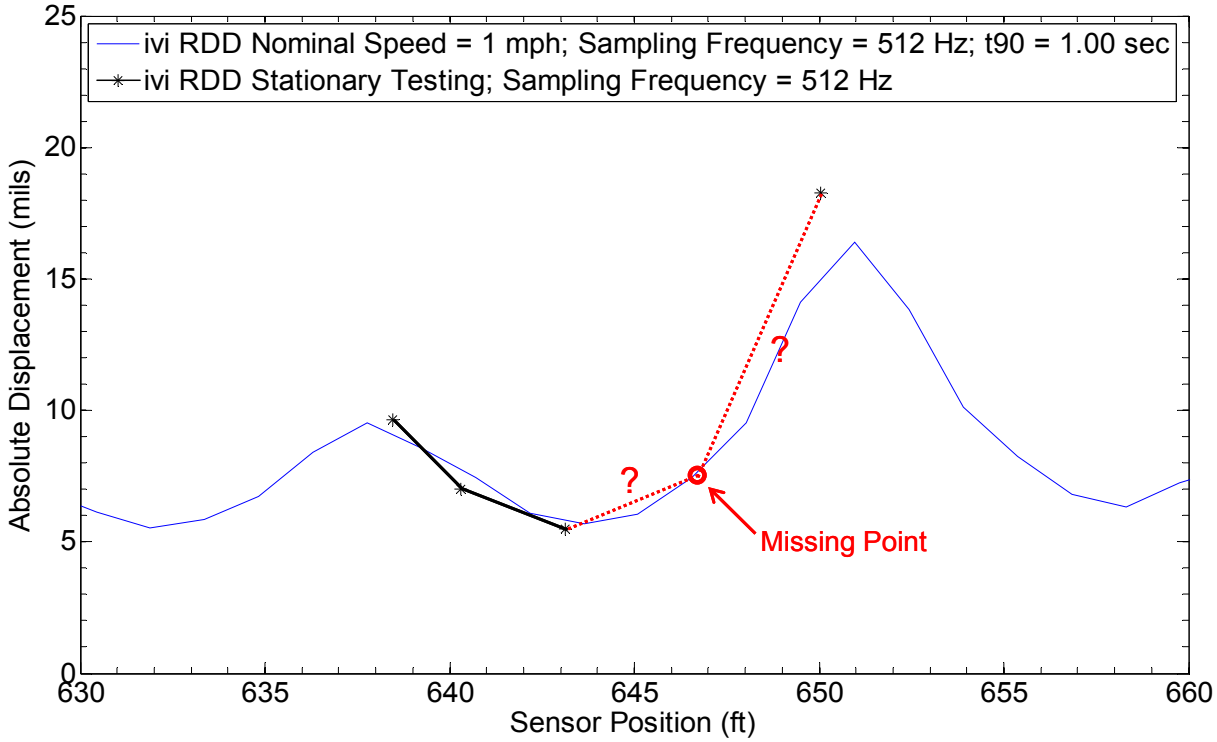

(a)

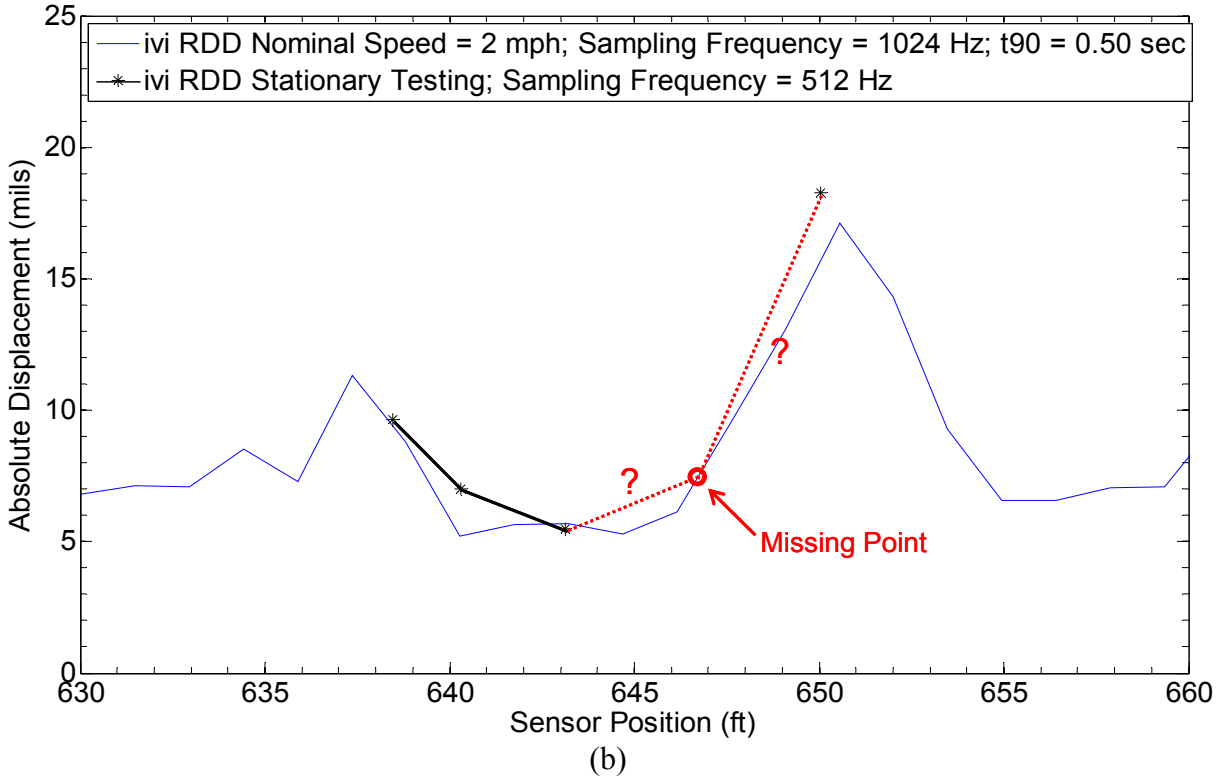

(b)

Figure 2.20: ivi RDD Deflection Measurements on Slab 43 (8-in. Slab): (a) Stationary and Testing Speed of 1 mph and (b) Stationary and Testing Speed of 2 mph.

2.8.6 Comparison of UT RDD and ivi RDD Continuous Deflection Profiles

The results of the continuous profiling along Path E with the UT RDD and ivi RDD are compared in this section. As already noted, the dynamic loading of the ivi RDD was not calibrated at the time of testing because no dynamic load cells were available. Thus, the load level of the ivi RDD along Path E is uncertain. For the purpose of comparison, the force level of the ivi RDD was adjusted by 75% to "equal" the force level of the UT RDD. The continuous deflection profiles with both machines when testing at a speed of 1 mph are shown in Figure 2.21. Both continuous deflection profiles show good agreement and the same trend in each deflection profile indicates lower deflections in the thicker slabs (16-in. thick slabs) and higher deflections in the thinner slabs (8-in. and 10-in. thick slabs), as expected.

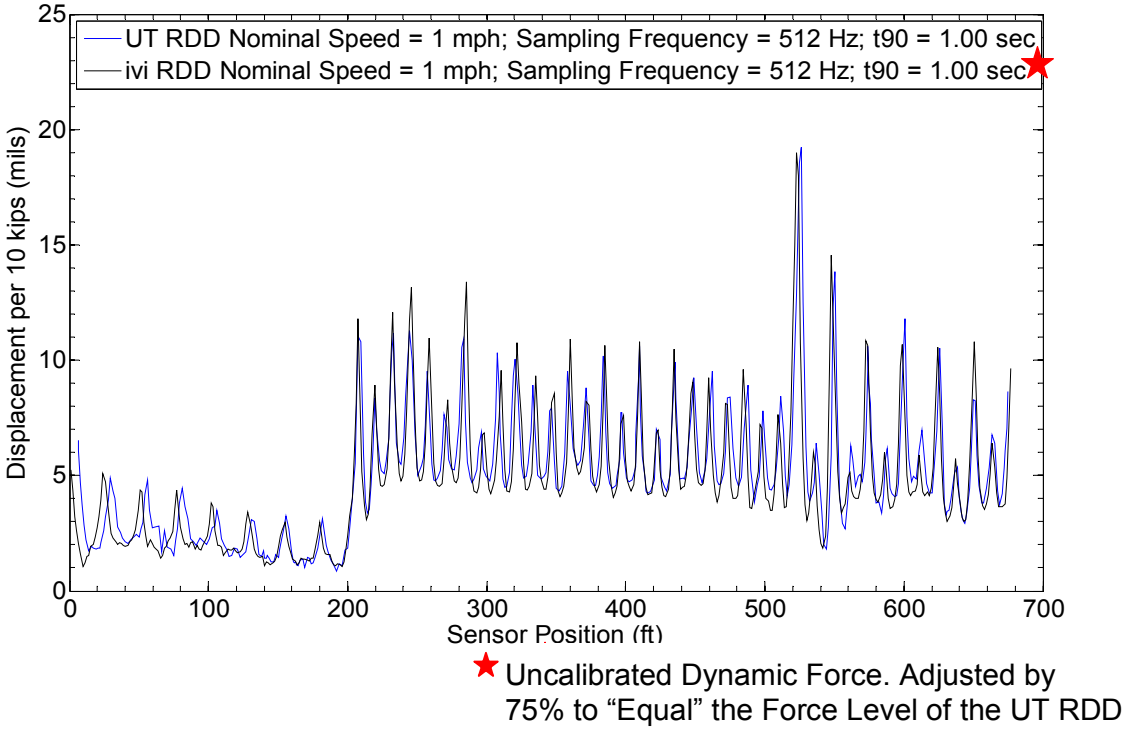

Figure 2.21: Comparison of UT and ivi RDD Deflection Profiles with Testing Speed of 1 mph.

2.9 Variations in Testing Speed during Profiling

The variation or uniformity in the testing speed during profiling was studied with both RDD devices while they profiled along Path E. Variations in the profiling speed can be a significant factor affecting the distance resolution in the RDD data because the "averaging" time (t90) is constant in signal processing. In particular, higher testing speeds near joints or cracks resulted in averaged deflections over longer distances, thus biasing the evaluation of the load-transfer condition to a better condition than actually exists. During testing, a distance encoder (rotary encoder) used to measure the distance traveled along Path E was attached to the rear wheel of the UT RDD. For measurements with the ivi RDD, the distance encoder was attached to the front wheel. Based on the recorded time and distance information, actual testing speeds were determined approximately every 6 ft (1.8 m). The testing speed of the UT RDD was manually controlled while the ivi RDD used a first-generation speed control system. Actual testing speeds

along Path E of the UT and ivi RDDs are shown in Figures 2.22 and 2.23, respectively. As seen in the figures, the ivi RDD had the better speed control at 1 mph, but both machines need to have improved speed controls, particularly at increased speeds.

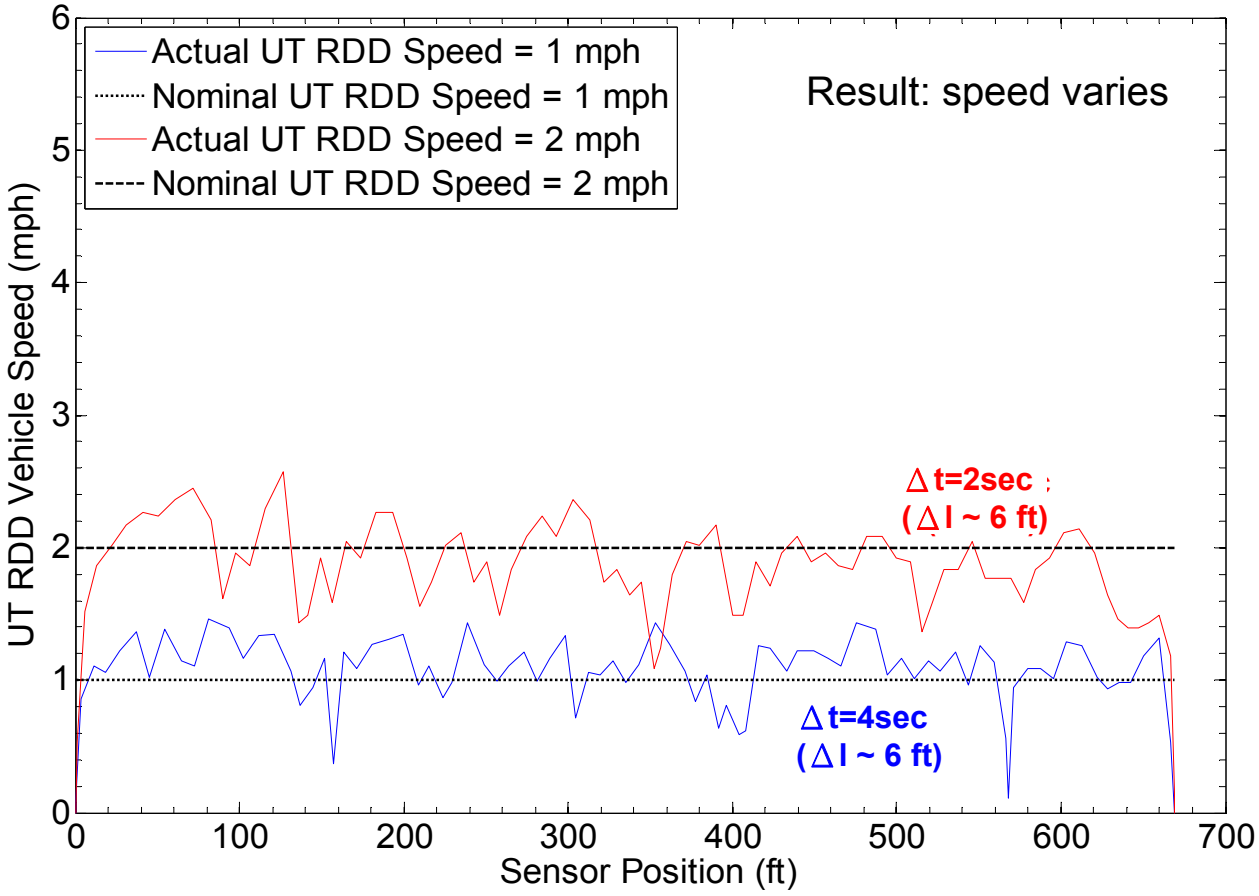

Figure 2.22: Nominal and Actual Testing Speeds of 1 and 2 mph Measured along Path E with the UT RDD

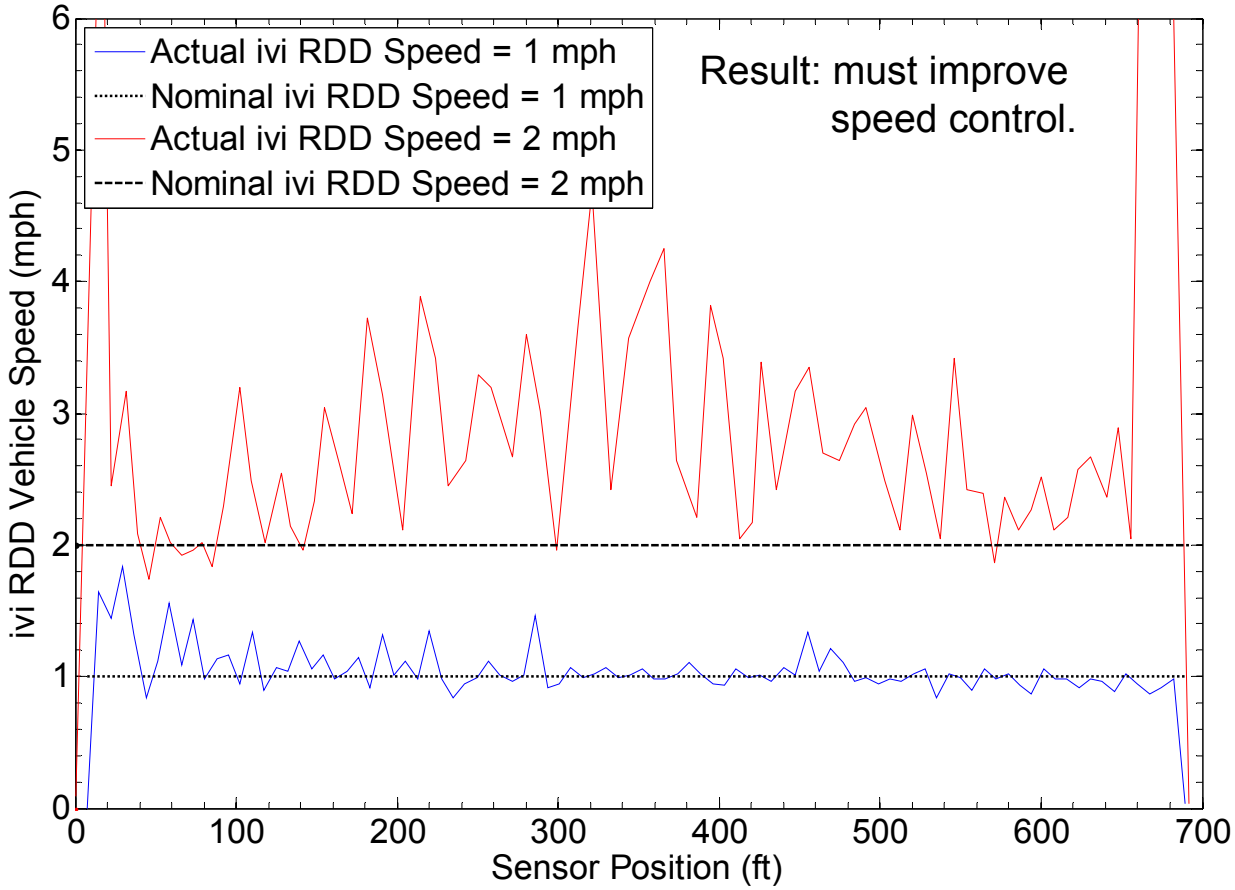

Figure 2.23: Nominal and Actual Testing Speeds of 1 and 2 mph Measured along Path E with the ivi RDD

2.10 Conclusions

Continuous profiling with the UT RDD and prototype ivi RDD was conducted along Path E at the TxDOT Flight Service Facility. Both devices were used to profile along Path E at a reference speed of 1 mph and then at several higher testing speeds. To verify these continuous measurements, stationary measurements with each machine were conducted at several discrete locations on one slab. Conclusions from the rolling and stationary measurements are summarized as follows:

UT RDD:

- Deflection profiles evaluated at 1 and 2 mph represented the pavement deflections and these measurements are typical of those found with the UT RDD in previous studies.
- At 3 and 4 mph, the deflection profiles became noisier, most likely due to poor stabilization of the rolling sensor and the associated carriage system.
- The stationary and rolling sensor measurements were in good agreement in the mid-slab area for testing speeds of 1 and 2 mph. However, the rolling sensor

measurements near the joints were somewhat smaller than the stationary measurements due to distance averaging associated with the rolling measurements.

ivi RDD:

- Deflection profiles evaluated at 1 and 2 mph represented the pavement deflections.
- At 3, 4, and 5 mph, the deflection profiles reasonably represented the deflections of the 8-in. thick slab. It is expected that the accuracy of these measurements will be improved with improved rolling sensors and testing speeds of 5 mph and more will be possible.
- The stationary and rolling sensor measurements were in good agreement at 1 and 2 mph.
- Higher (but uncertain) dynamic forces were applied with the prototype ivi RDD. This situation will be changed in the next version of the system.
- A different hold-down system for the rolling sensor changed the calibration factor of the sensor compared with the UT RDD.

Overall, these tests and the associated comparisons were very successful. The opportunity to experiment with a prototype device like the one built by Industrial Vehicles Incorporated greatly assisted the CTR and TTI research team and TxDOT Project Monitoring Committee (PMC) in moving forward with developing the TPAD specifications. The ivi prototype RDD allowed the basic configuration of the TPAD to be readily envisioned and needed improvements were readily identified.

Chapter 3. Improved Rolling Sensors and Associated Analysis Tools

3.1 Introduction

The Center for Electromechanics (CEM) under direction of the Center for Transportation Research (CTR) at UT is developing advanced sensor technology and analysis tools under Task 4 of Project 0-6005. The primary technical objective is to develop sensor technologies which facilitate continuous pavement deflection measurements at speeds in the range of 5 to 10 mph. Fundamental to this objective are the abilities to: (1) discriminate between background noise and sensor signal at frequencies of 30 to 100 Hz (primarily at 30 Hz) and (2) maintain sensor contact with the pavement during negative acceleration associated with pavement variations and pavement deflections. In order to accomplish these tasks, CEM is developing a Dynamic Analysis and Design System (DADS) model of the proposed TPAD vehicle (using the original RDD as an example), Vibroseis roller system, sensor array carriage, and rolling sensor system to evaluate current system dynamics and explore concept system performance.

3.2 DADS Model of the RDD

CEM has completed the DADS model of the RDD vehicle in its current state. To facilitate construction of the DADS model, a SolidWorks model was developed for the RDD sensor array carriage, rolling sensor, Vibroseis roller system, and the truck. Figure 3.1 and Figure 3.2 show the DADS and SolidWorks models, respectively. In addition to modeling the current sensor array system, an alternative sensor carriage array was developed in SolidWorks as shown in Figure 3.3 and Figure 3.4 (note: the chassis is hidden in these figures to enhance the clarity of the modifications). This model in SolidWorks was incorporated into the DADS model. The alternative concept attempts to address assumed limitations of the previous system through incorporation of better isolation from the RDD chassis (and hence the TPAD chassis) and provides provisions for inclusion of active suspension to stabilize the sensor carriage. CEM has demonstrated operation of the model on randomly generated pavement surface models and is gathering typical pavement profile data to perform comparisons with actual RDD dynamics.

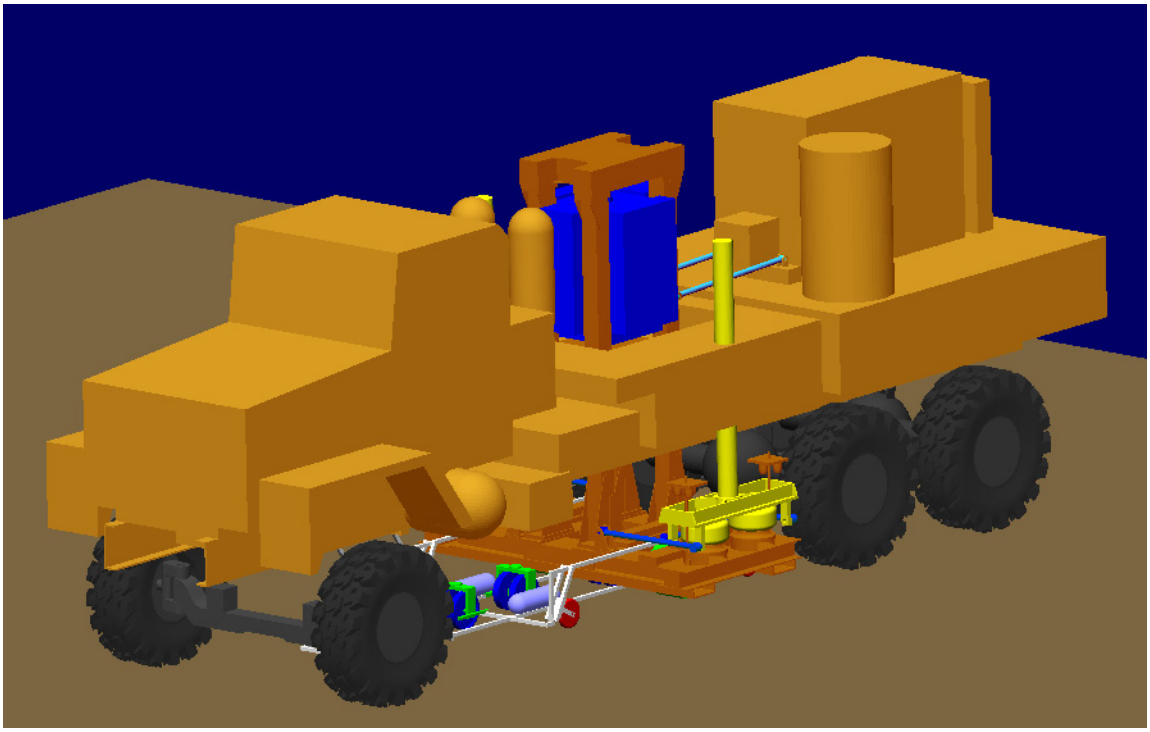

Figure 3.1: DADS Model of the RDD

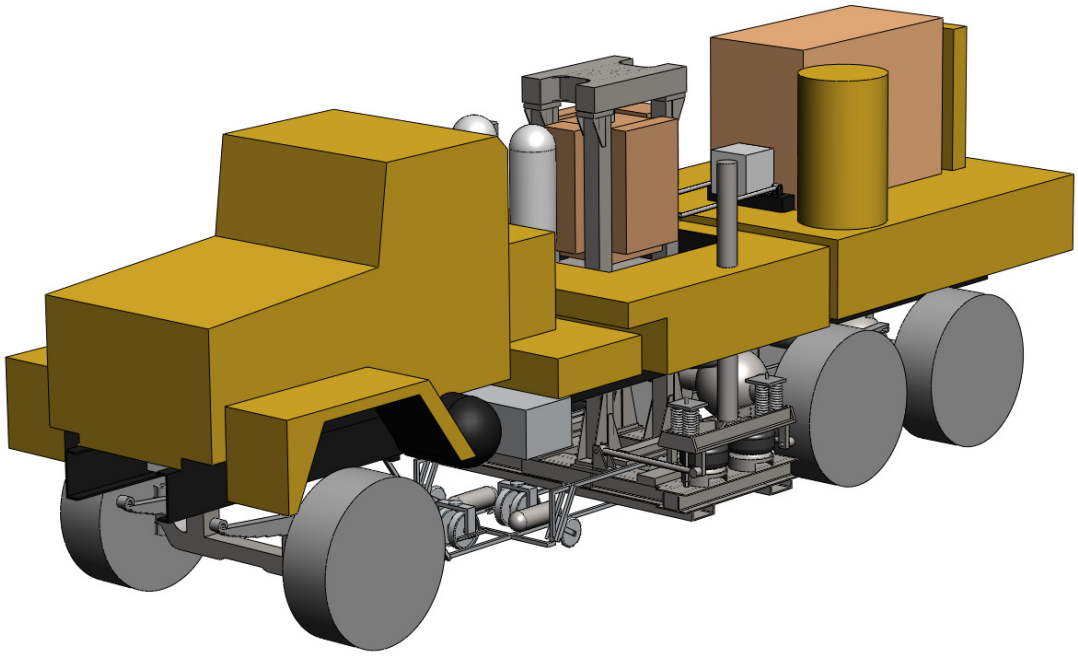

Figure 3.2: SolidWorks Model of the RDD

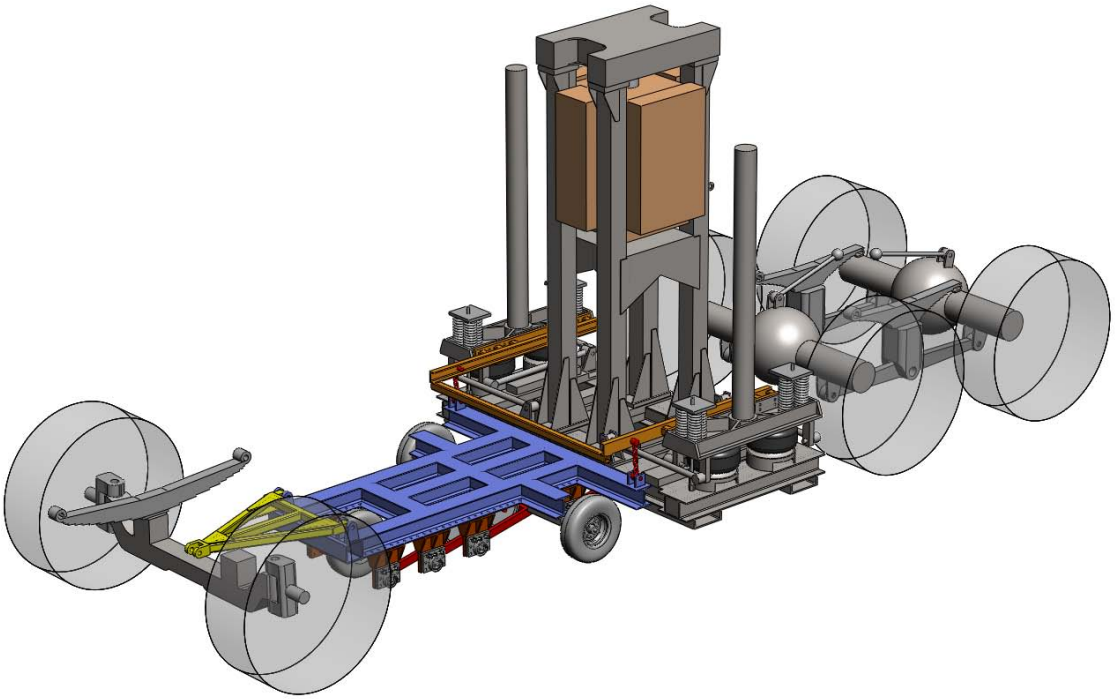

Figure 3.3: SolidWorks Model of Modified RDD Sensor Carriage from top

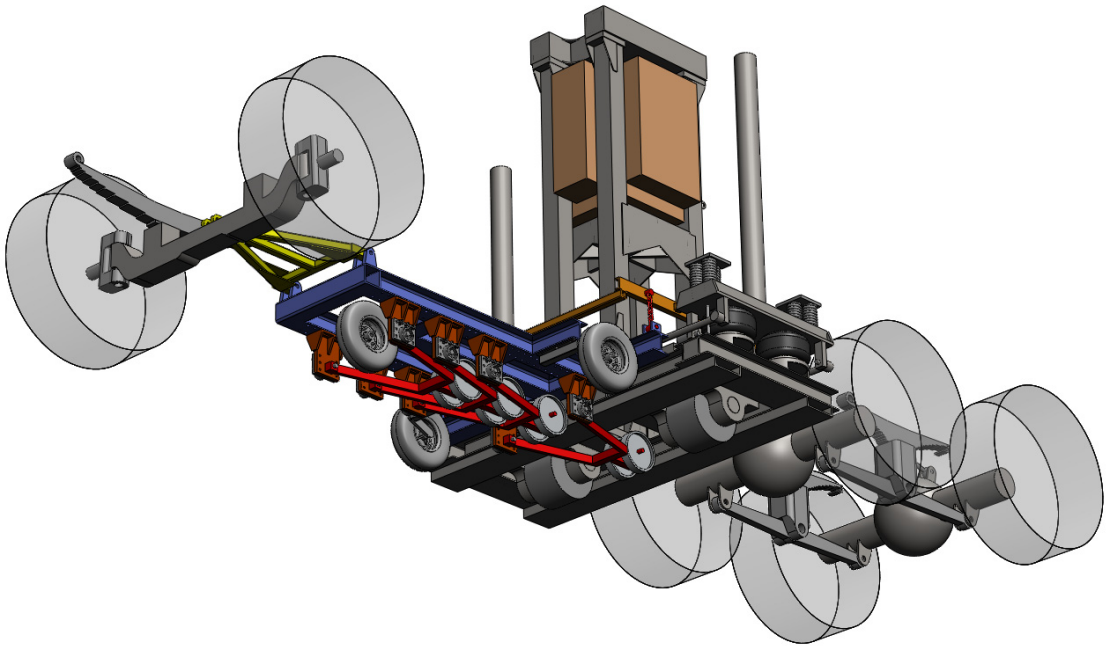

Figure 3.4: SolidWorks Model of Modified RDD Sensor Carriage from bottom

3.3 Transfer Function Models of the Rolling Sensor System

In parallel with development of the DADS model, CEM has developed transfer function models for the sensor array carriage and sensors. These linear models have been used to develop fundamental insights into the sensor array carriage dynamics that are often not obvious from the detailed DADS models. Two systems were examined: System 1 assumes the carriage is supported by the transducer wheels alone and System 2 assumes the carriage is supported by secondary tires in addition to the transducer wheels. Figure 3.5 shows these two systems schematically. In the systems, the movements stiffnesses, damping rates, and masses are denoted as follows:

Movements
y_G – Vertical displacement component of the ground
y_W – Vertical displacement component of geophone transducer cart wheel
y_C – Vertical displacement component of guide carriage for geophone transducer cart array.
y_T – Vertical displacement component of geophone transducer mass

Stiffnesses
K_W – Spring rate of geophone transducer cart tire/wheel
K_S – Spring rate between guide carriage for geophone transducer cart array and transducer cart.
K_T – Internal spring rate of geophone transducer
K_{S2} – Tire/Wheel spring rate of guide carriage for geophone transducer cart array.

Damping Rates
B_W – Damping rate of geophone transducer cart tire/wheel
B_S – Damping rate between guide carriage for geophone transducer cart array and transducer cart.
B_T – Internal damping rate of geophone transducer
B_{S2} – Tire/Wheel damping rate of guide carriage for geophone transducer cart array.

Masses
M_{wheel} – Mass of geophone transducer cart tire/wheel
$M_{carriage}$ – Mass of geophone array guide carriage
$M_{geophone}$ – Geophone reference mass.

It was assumed that the dynamic behavior of the geophones in the rolling sensors have a negligible effect on the behavior of the rest of the system (due to relatively small geophone mass), thus the geophone output then is the product of wheel displacement as a result of pavement displacement with the geophone response transfer function. Eliminating the geophone from system dynamics leads to two simplified systems as shown in Figure 3.6.

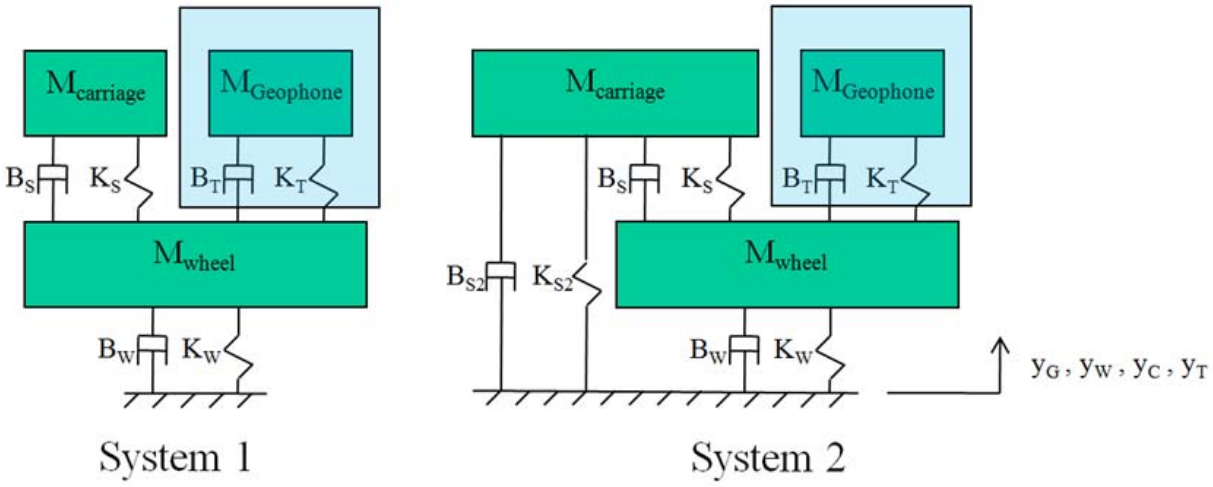

Figure 3.5: Transfer Function Models of Rolling Sensors and Sensor Array Carriage

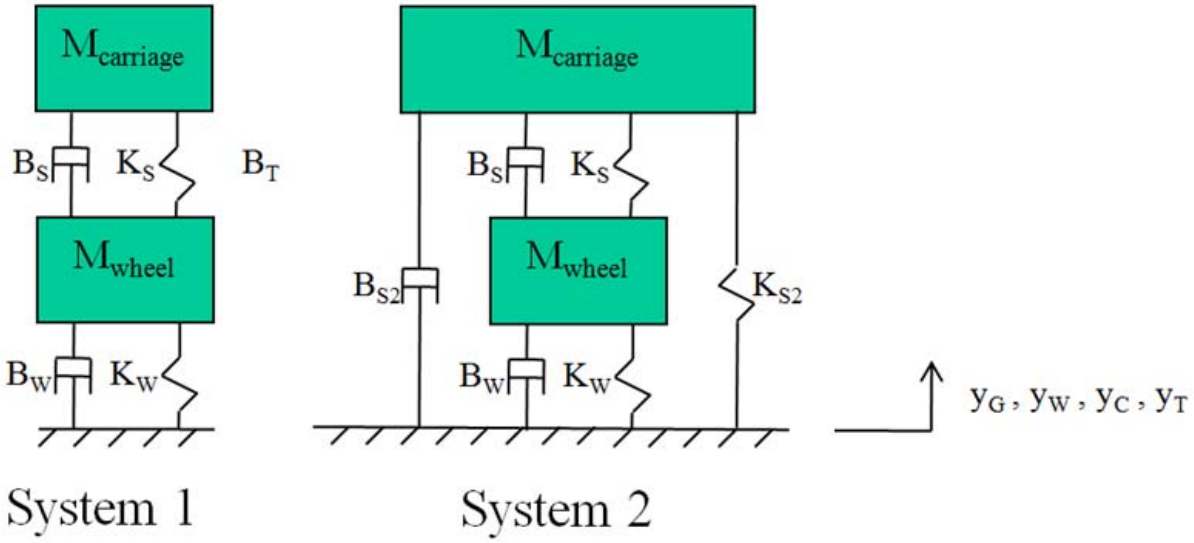

Figure 3.6: Simplified Transfer Function Models

For small deflections, a linear behavior is probably valid for the air springs and tires associated with the rolling sensors. One noteworthy discrepancy that this modeling approach omits is that the carriage tire location and transducers are not spatially coincident on the real hardware. Understanding this potential limitation, the analysis was performed assuming the same pavement input to tires and transducer in order to reveal trends. From these transfer function models, the operational frequency spectrum at which the rolling sensor amplitude response can be expected to match the pavement amplitude was determined.

System 1 and System 2 (Figure 3.6) both result in 4th order transfer functions for Y_W with respect to Y_G. For both systems, spectral input interacting with the carriage natural frequency would be undesirable in terms of keeping the transducer on the ground and spectral input above

the transducer natural frequency results in loss of signal amplitude response. The transfer function for System 1 (Figure 3.6) is expressed by Equation 3.1.

$$\frac{Y_W}{Y_G} = \frac{(sB_W+K_W)}{\left[s^2\left(M_{wheel}-\left[\frac{B_S^2}{(s^2M_{Carriage}+sB_S+K_S)}\right]\right)+s\left(B_W+B_S-\left[\frac{2B_SK_S}{(s^2M_{Carriage}+sB_S+K_S)}\right]\right)+\left(K_W+K_S-\left[\frac{K_S^2}{(s^2M_{Carriage}+sB_S+K_S)}\right]\right)\right]} \quad 3.1$$

The terms in orange are only affiliated with the Carriage and for omega much greater than sqrt($K_s/M_{Carriage}$), they approach zero, resulting in the simplified transfer function for System 1 as expressed by Equation 3.2.

$$\frac{Y_W}{Y_G} = \frac{(sB_W+K_W)}{[s^2M_{wheel}+s(B_W+B_S)+K_W+K_S]} \quad 3.2$$

As a result, over the frequency spectrum:

$$\text{sqrt}(K_s/M_{Carriage}) << \text{omega} << \text{sqrt}[(K_W+K_s)/M_{Wheel}] \quad 3.3$$

the transducer wheel amplitude response matches that of the pavement. Similarly, for System 2 (Figure 3.6), for omega much greater than sqrt[$(K_s+K_{s2})/M_{Carriage}$] and $B_S << M_{Carriage}$, the resulting transfer function is the same as shown in Equation 2 above. As a result over the frequency spectrum:

$$\text{sqrt}[(K_s+K_{s2})/M_{Carriage}] << \text{omega} << \text{sqrt}[(K_W+K_s)/M_{Wheel}] \quad 3.4$$

the transducer wheel amplitude response matches that of the pavement. It is important to note that amplitude response matching the pavement input does not necessarily indicate that wheel lift off will not occur. To insure wheel lift off does not occur over the operating range one needs to apply specific rules set forth by Stokoe and Bay, 1998.

The desire to have carriage natural frequency low presents a challenge to reduce friction as much as possible, which is consistent with the CTR-developed custom low durometer and low pressure air spring. Additionally, the desire to make the sensor wheel/tire natural frequency much higher than pavement excitation frequency is aided by the additional spring rate provided by the air spring.

3.4 Path forward in Second Year

CEM's path forward during the next phase of the project combines working closely with CTR to better understand rolling noise sources while continuing development of other alternative sensor array concepts. These design concepts will be evaluated and prototype candidates will be selected for fabrication and testing by CTR. It is envisioned that the design and testing may include one or more iterations. Some of the opportunities for improvement under current consideration are (1) wide compliant sensor tires, (2) integrating a sensing mechanism into the loading rollers, (3) replacing or supplementing geophones with an inertial measurement system stabilized with an active suspension system, and (4) the use of an external analog integrator of the

geophone signal. Some opportunities for improvement of the sensor carriage structure and vehicle attachment to reduce resonant vibration and transmitted vibration from the truck are also under consideration. Specific areas of current interest are the fundamental sources of the road–tire noise and vibration generation, and what efforts can be made to reduce their severity.

Chapter 4. Improved Signal Processing of Rolling Sensor Output

4.1 Introduction

The primary activities associated with TPAD's signal processing during the first project year are discussed below. This work is conducted as part of Task 4 in Project 0-6005. In brief, several modifications were made to the existing RDD processing code to accommodate the requirement for an increased rolling speed, as well as to provide for more accurate demodulation and denoising procedures.

4.2 Higher Sampling Frequency Rates

A primary goal of the CTR activities during the first year was to study the effect that increased testing speeds required for the TPAD will have on signal acquisition and processing of the rolling sensors. To this end, we adapted the signal processing capabilities associated with the original RDD, to accommodate the demands imposed on the processing by TPAD's increased testing speed. Specific steps taken included:

1. Software migration to a more widely adopted platform: The data analysis procedure for the TPAD is based on the generalized procedure already in use with the original RDD. Within the last six months, the first improvement to the RDD procedure was a transition to Matlab-based programming. After data acquisition using LabVIEW, binary data files are processed with a series of newly programmed Matlab functions. These functions replicate the RDD processing, initially developed using the less broadly used IGOR Pro. The new Matlab functions read the binary data, separate the data into individual raw force and raw displacement vectors, filter and de-noise the data, and produce displacement profiles normalized to a 10-kip load.
2. Requirements for increased testing speed: To allow increased rolling (testing) speed, without sacrificing data accuracy, we adhered to two basic empirical rules which are: a) a minimum of 12 data points per wavelength is required to ascertain a minimum quality on the reproduced waveforms, and b) the acquisition rate/sampling frequency should be increased proportionally to the rolling velocity.
3. Study effect of sampling frequency: After developing the Matlab code, studies were performed to determine the effect of changing the sampling frequency. For example, Figure 4.1 shows two displacement profiles created from data collected with the original RDD along lane C63 at the TxDOT Flight Service Facility. Other than a change in the data acquisition sampling frequency, all other analysis parameters were kept constant. As can be seen, the resulting profiles are very similar, with the difference that the higher sampling frequency seems to improve the resolution. Figure 4.1 is fairly representative of the signal processing experiments we conducted resulting from the increase in the sampling rate.

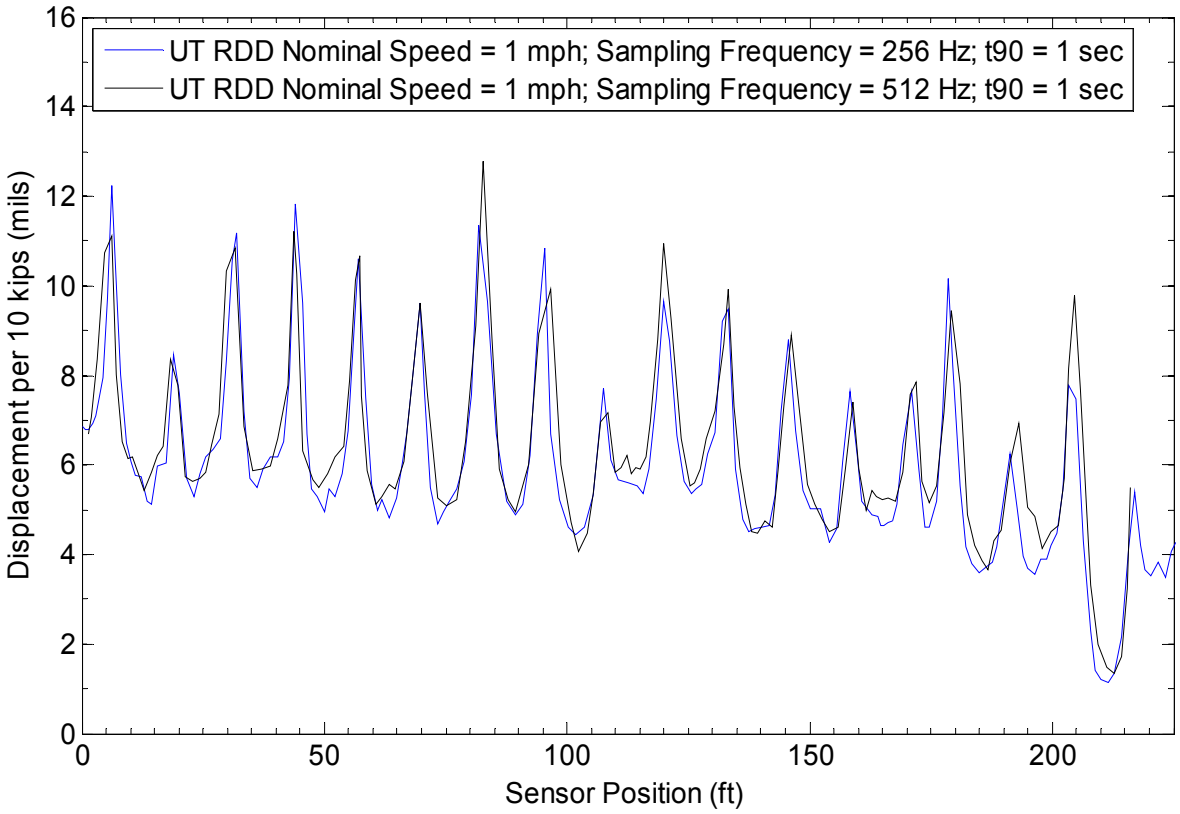

Figure 4.1: Displacement profiles of lane C63 at ABIA created with data sampling frequencies of 256 Hz and 512 Hz.

It was, therefore, concluded that changing the sampling frequency of the data collection would not adversely affect the displacement profiles produced through the data analysis procedure.

4. Analyze records with increased testing speeds: Next, a series of experiments were conducted, in which the rolling speed was increased and the sampling rate was also proportionately increased. We were interested in recovering displacement profiles that would exhibit the same level of accuracy. Figures 4.2 to 4.4 show displacement profiles created with data collected from the FSF testbed.

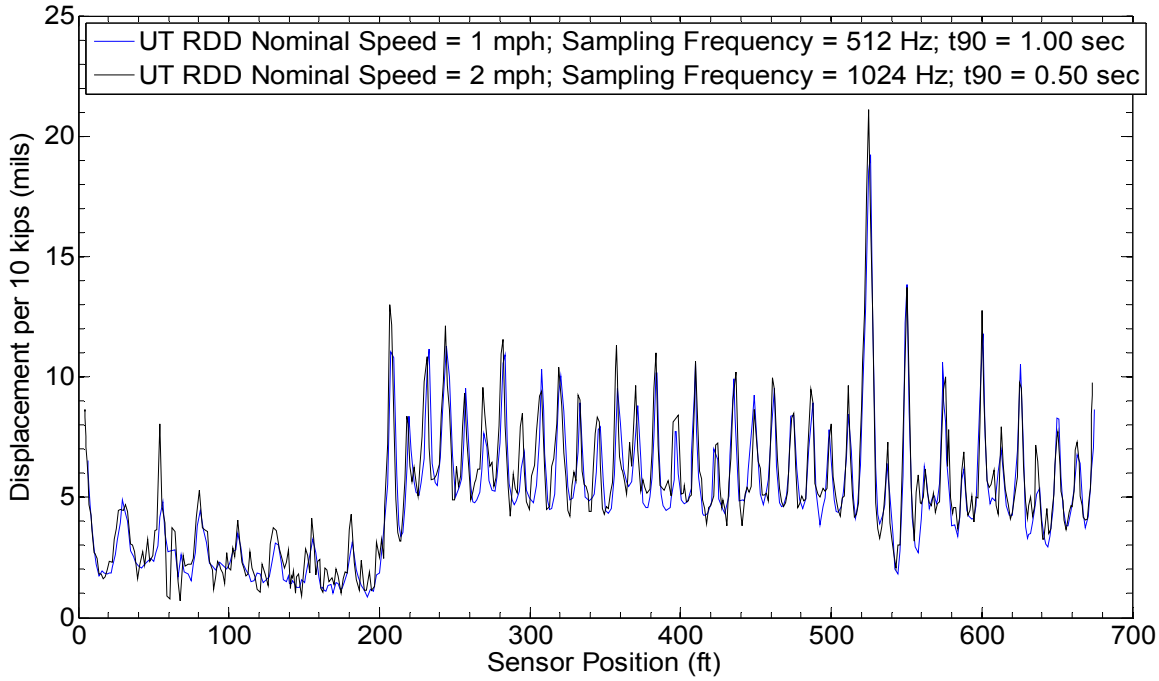

Figure 4.2: Displacement profiles at the FSF testbed created with vehicle speeds of 1 and 2 mph and data sampling frequencies of 512 Hz and 1024 Hz, respectively.

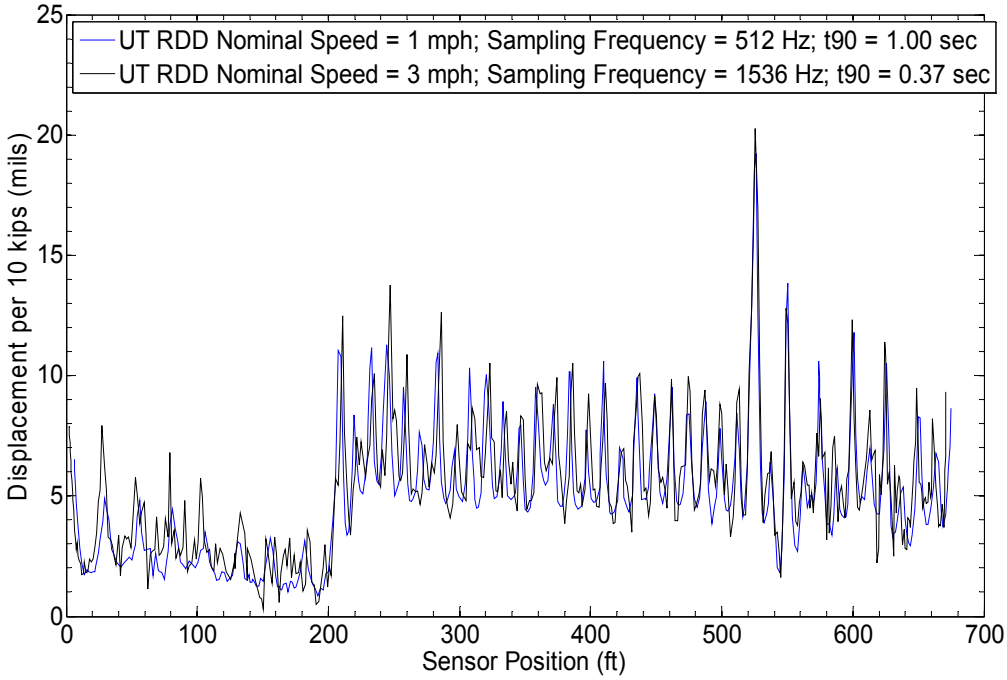

Figure 4.3: Displacement profiles at the FSF testbed created with vehicle speeds of 1 and 3 mph and data sampling frequencies of 512 Hz and 1536 Hz, respectively.

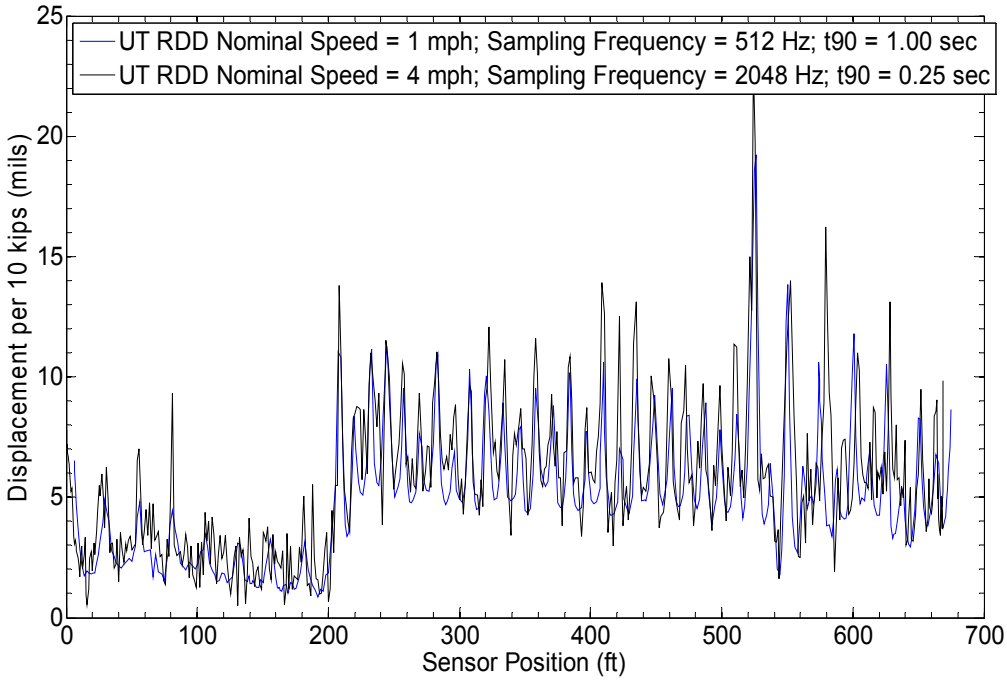

Figure 4.4: Displacement profiles at the FSF testbed created with vehicle speeds of 1 and 4 mph and data sampling frequencies of 512 Hz and 2048 Hz, respectively.

It can be seen that the joints are clearly identifiable, irrespective of the rolling speed. Testing with the prototype ivi RDD (discussed in Chapter 2) showed identical trends, allowing the same conclusion to be drawn regardless of the vehicle being operated. Whereas, Figures 4.2 and 4.3 show good agreement at the displacement peaks between the different velocities, differences at the peaks are discernible in Figure 4.4 when the velocity contrast is higher. At the moment, we hypothesize that the higher sampling rate allows for displacements to be collected closer to the joints, and therefore, the joint's displacement appears higher at higher sampling rates; we are also considering alternate interpretations and intend to perform additional studies to determine the answer.

4.3 Lower Sampling Frequency Rates

Alternative to increasing the sampling frequency as TPAD's rolling speed is increased, we also investigated the potential for using sinc interpolation to recreate missing data points in the raw force and displacement vectors, while keeping the sampling rate lower. The additional data, combined with data collected at lower sampling rates was then filtered and the associated displacement profiles were created. Figure 4.5 shows a sample of a raw total force waveform, originally sampled at 512 Hz with the UT RDD, and then modified by sinc interpolation to a sampling frequency of 2048 Hz. As shown in the figure, there is very little clarity or smoothness gained from the sinc interpolation procedure. Because the procedure is very computationally expensive, we have concluded that it would be unwise to include it in the TPAD's data processing.

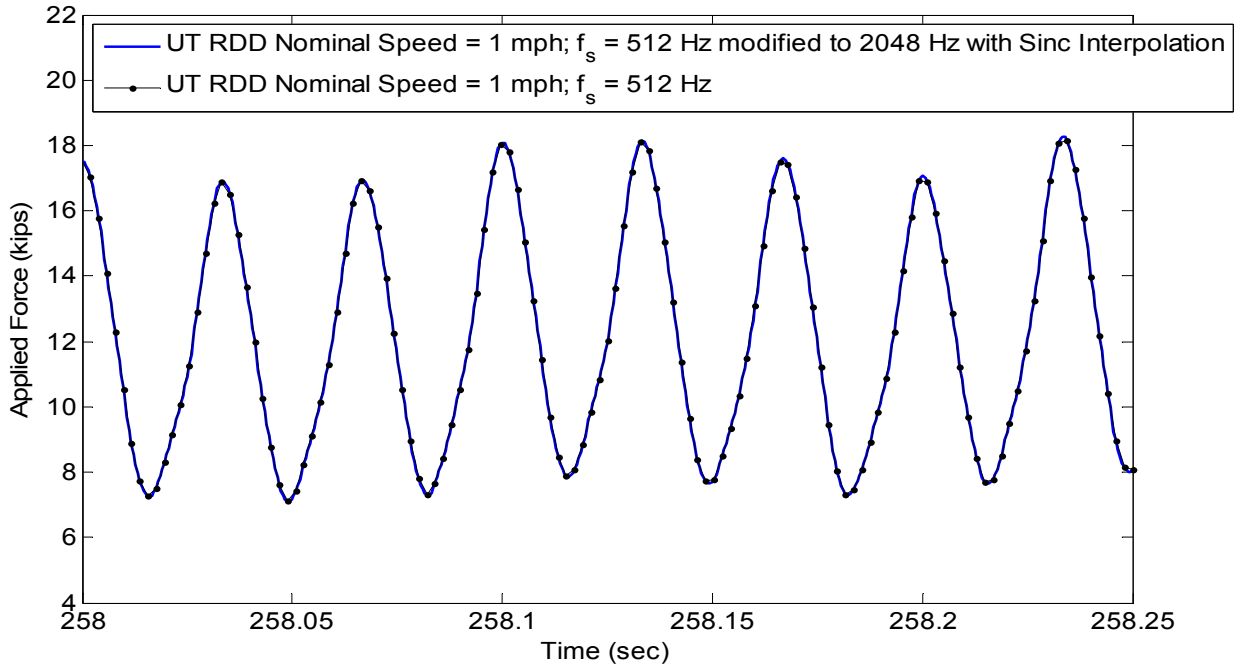

Figure 4.5: Raw force vector, sampled at 512 Hz with the RDD and then modified to mimic a sampling frequency of 2048 Hz.

4.4 Loading Frequency Implications

A secondary investigation on the difference between the frequency of the on-board oscillator of the RDD and the demodulation oscillator used in processing the RDD data was also carried out. It can be shown that if these two frequencies vary by more than 0.5% to 1.0%, then significant errors, 12.5% and 30%, respectively, will result in the filtered output and therefore, the displacement profiles as well. Current RDD data processing uses a user-input operating frequency to control the demodulation oscillator used to filter and de-noise the raw force and displacement data that are collected. Theoretically, the user will input the exact same frequency that was used by the RDD's on-board oscillator (also user-specified in the data collection process) when the raw data are collected. However, due to small errors in the RDD's function generator which creates the on-board oscillator's waveforms, the waveforms used to generate the RDD's operating frequency may have a frequency slightly different than the user-specified frequency. This would, in turn, create a difference between the on-board oscillation used to collect the data and the demodulation oscillation used to filter the data. We note that this difference would also affect the peak displacements.

Through Fourier transforms of the raw force data collected by the RDD, the actual on-board oscillator frequency was found to vary less than 0.2% from the user-specified demodulation frequency during the most recent experimental studies. Therefore, a minimal error results in the final, filtered output data. This error would be further minimized, however, by using the exact on-board oscillator's frequency as the filter's demodulation frequency. To this end, a new Matlab function was written to perform a Fourier transform on the raw force data collected by the TPAD. The peak frequency in this transform is considered the actual on-board oscillator's frequency, and it will be used as the filter's demodulation frequency in future TPAD data processing to minimize error during the filtering procedure. Finally, a warning will also be output

to the user if the user's input operating frequency varies by more than 5% from the peak frequency in the raw force data.

Chapter 5. Status of the TPAD Data Acquisition System Development

5.1 Introduction

In study 0-6005, the next generation rolling dynamic deflectometer (RDD) system, which is referred to as the TPAD, has been developed under a joint research study funded by TxDOT with researchers from both the Center for Transportation Research (CTR) and the Texas Transportation Institute (TTI). TTI is responsible for the development of an integrated data acquisition and display system. The new generation TPAD will include many sensors serving a variety of functions; a schematic of the proposed system is shown in Figure 5.1. The most important sensors include:

1) a series of rolling geophones that measure pavement deflections under a sinusoidal loading system,
2) a load cell or accelerometer for measuring dynamic loads on the pavement surface,
3) a video camera system for documenting roadway conditions,
4) a distance measuring device, and
5) a Ground Penetrating Radar (GPR) system for documenting subsurface conditions

In the first year of this study a prototype laboratory-based data acquisition system was designed and developed under Task 5. This system is described in this chapter. In year 2 the proposed system will be field tested by integrating it into the operational UT RDD field unit. This will provide TTI with the opportunity to field test and improve the system before incorporating it into the new TPAD system.

5.2 Factors that Influence the Data Acquisition

Before starting the software coding, it is important to develop a plan that will direct the system development. For the final TPAD field data acquisition software, the main functions are:

- collect multiple types of sensor signals and save them to disk,
- develop a compact data format to save the potentially very large data sets,
- try to use a one-touch screen computer to control the running of the system, and
- have real time displays for the TPAD operators to review data during acquisition.

TTI has overall responsibility for integrating the data. However, at the current time, the responsibility for the individual sensors is as follows: TTI is in charge of the GPR, digital video, and GPS devices; CTR is responsible for the rolling sensor geophone signals; and the equipment supplier is responsible for load, distance measurements, and vehicle speed information. In the current prototype system, TTI will also collect raw geophone data. The final form of the system will be developed in coordination with the UT team.

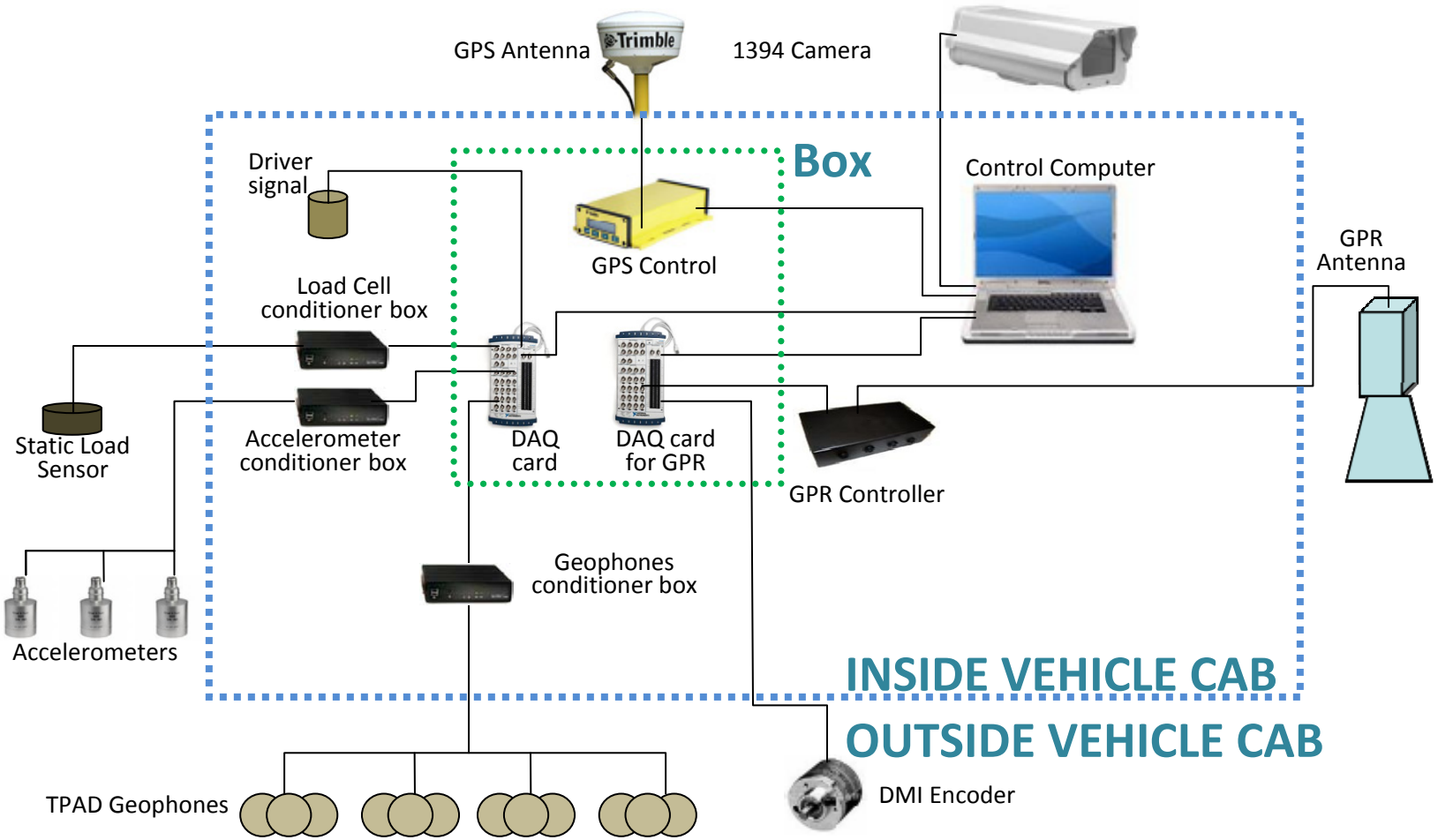

Figure 5.1: TPAD Data Acquisition System Hardware Setup

Table 5.1 lists all the sensors that will be gathered and integrated into the final TPAD data acquisition system. From this table, we noticed that three kinds of devices are needed to collect these signals:

- analog-to-digital data acquisition card,
- IEEE 1394 digital video acquisition card, and
- serial port (or COM port) for GPS data acquisition.

The IEEE 1394 and COM ports are available on most computers. So for this study, we only need to purchase an analog to digital data acquisition card. One potential problem is that for the majority of data acquisition systems, no matter how many channels they collect, they only operate on a single time basis. This means that any DAQ card can only set one data collection rate. However, different rates are required for the TPAD data integration system. Only GPR needs a high data acquisition rate (around 100KS/s for each channel, with a total of four channels), and the other sensors operate at much lower rates (typically 1 to 1000Hz).

Table 5.1: Sensor List of Proposed TPAD System

Sensors	Requirement	Organization
DMI encoder	Repeatable, resolution to 1 inch.	TPAD Manufacturer
Geophones	1000 Samples/second, maximum of 4 geophones, Time mode data acquisition.	CTR
Accelerometers	1000 S/s, around 4 accelerometers. Time mode.	TPAD Manufacturer
GPR	Need 4 channels DAQ card which can handle at least 100kS/s. distance mode, 1 trace per foot.	TTI
Digital Video	5 feet per frame, video resolution is set as 640X480. IEEE 1394 firmware camera is used.	TTI
GPS	1 point per second, sub-meter accuracy. For the horizontal location, 8 decimal point accuracy will be needed.	TTI
Surface IR temperature	One measurement per foot, distance mode.	TTI
Driving signal	Indicate the speed of the vehicle. Save the average speed for every foot.	TPAD Manufacturer
Static load sensor	Monitor the static load roller pressure on the pavement surface at 50 S/s, time mode.	TPAD Manufacturer

In addition, some of the signals such as GPR need to be collected in the distance mode, which means the data are collected at a fixed interval, say every 2 feet. In this case if the vehicle stops at a traffic light then the data acquisition stops. Other types of signals (geophones) are collected in the time mode, which means whether the vehicle moves or not, the signals are collected at a constant rate. From the above table (Table 5.1), DMI, geophones, accelerometers, and GPS are in time mode. All others are distance based.

Based on the above discussion, it is difficult to collect all the required data using only one data acquisition card. Therefore, it is proposed to use two cards in our field data acquisition plan: one will be for the fast GPR DAQ card; for this we have purchased the NI-9215A USB 4 channel 100KS/s rate card made by National Instruments. A second card will be used for the low rate signals. This card is a NI-9218 BNC, 16 channels, BNC connection, and differential wired mode.

5.3 Storage Requirements for Different Data Formats

A good data storage format is very important for this TPAD project. The following example provides an estimate of the amount of data which will be collected in a typical 5-mile long TPAD survey. The estimated size of the data files with different storage formats is shown in Table 5.2.

Table 5.2: File Size Estimate of TPAD System

						Binary format	
Sensor	**Channel**	**Rate**	**Test mode**	**Total Number of data points**	**ASCII Format**	**4 Bytes float**	**2 Bytes float**
DMI encoder	1		Distance	26400	316800	105600	52800
Geophones	4	500	Time	864000000	10368000000	3456000000	1728000000
Accelerometers	4	500	Time	864000000	10368000000	3456000000	1728000000
GPR	3	trace/ft	Distance	81100800	973209600	324403200	162201600
Digital Video	1	1frame/2ft	Distance	396000000	4752000000	1584000000	792000000
GPS	1	1 /s	Time	4320000	51840000	17280000	8640000
Surface IR temperature	1	1/feet	Distance	26400	316800	105600	52800
Driving signal	2	4 /s	Distance	1728000	20736000	6912000	3456000
Static load sensor	2	500	Time	432000000	5184000000	1728000000	864000000
			Total	2643201600	31718419200	10572806400	5286403200
			Total (Gb)		31.718 Gb	10.573 Gb	5.286 Gb

The following assumptions were used to make these estimates. If the test mode is time, the calculation is based on the TPAD average testing speed of 1 mile/hour. If the saved format is ASCII, each floating number is saved as 10 digits plus two spaces.

Currently, binary format is widely used for storing big files. The benefit of binary format is that the speed of both saving and reading the data are much faster than for the ASCII format, and a much smaller file size is required. In Table 5.2, two columns are listed for binary format: one is for the high precision double accuracy real numbers (each number takes 4 bytes or 32 bits); the other one is for floating numbers, which take 2 bytes for each number.

In all calculations, it is assumed that the vehicle travels at a constant speed without stopping. But in actual testing, stopping always occurs for traffic signals, lane obstructions or hardware/software malfunctioning. Therefore, these size estimates are at the low end and the actual file size may be larger.

From Table 5.2, five miles of data will take about 5.3 Gb disk space, assuming that the vehicle travels at 1 mile/hour. If the vehicle speed is 3 miles/hour, the file size will reduce to 2.4 Gb. File sizes around 2.4Gb are acceptable for both the post processing and copying or reading the data.

It is proposed that the floating binary format will be used for the TPAD project. The format details will be discussed in a future report.

5.4 Simulator Software Development

TTI will be in charge of integrating data generated from all sensors, which also includes the sensors provided by the TPAD manufacturer and CTR that monitor functions under their purview. This effort will be a challenging task. To accelerate the software development, it is proposed that a prototype system be developed in the laboratory prior to installing it in the field. In year 1 of this study, a pilot lab system was developed as described below.

To facilitate this development, TTI purchased one analog output DAQ card with simulation capabilities. These simulation capabilities mean that existing sensor data can be sent from another computer and presented to the DAQ as if it were new field data. This package with a combination of real and simulated data ensures that the data acquisition and display system can be completely developed and tested in the laboratory. The current program can simulate the following signals:

- GPR radar signal and trigger signal,
- DMI signal, and
- GPS signal (using a serial port).

TTI has already obtained two sets of TPAD geophone data from CTR, but we are still working on a vibratory setup to generate simulated TPAD geophone signals. We recently built the device shown in Figure 5.2 to create these signals.

At this moment we do not have input data from typical sensors associated with the TPAD such as accelerometers, vehicle speed, and static load. Therefore, we plan to simulate their signals in the next stage of the coding.

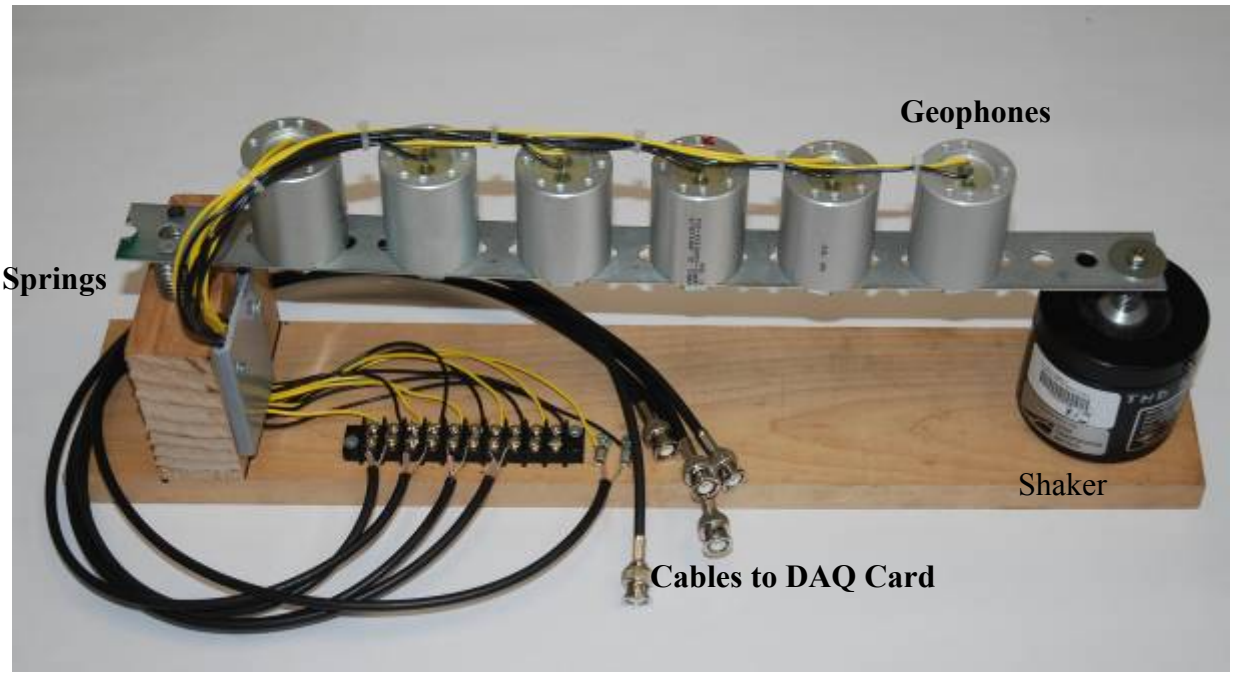

Figure 5.2: Simulator of Multiple Geophone Outputs

Figure 5.3 shows the TTI work space for this TPAD project. One computer is used to simulate several of the signals while the geophones and video data are real data captured in real time. The other main computer is in charge of data collection.

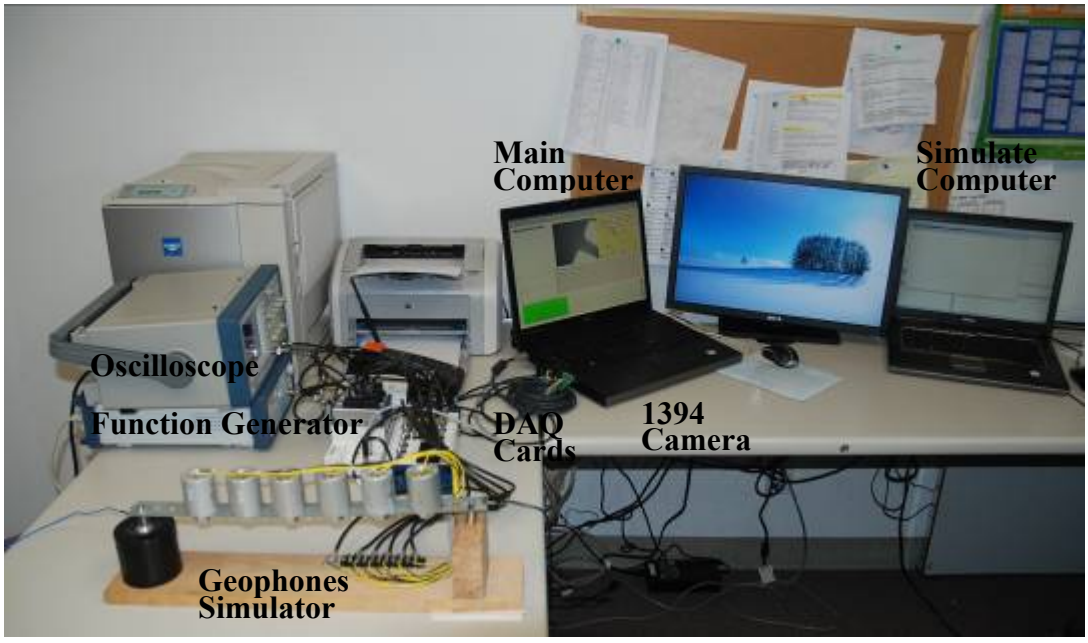

Figure 5.3: TTI Laboratory Simulation Set Up for the TPAD Project

5.5 Data Acquisition Software Development

TTI's current GPR system uses two computers: one for GPR data, another one for video collection. The proposed TPAD system will have many additional sensors and it will most likely require two data acquisition cards. However, in this prototype system, we plan to determine if it is feasible to collect all data with a single computer setup. The computer program described below was coded to try to determine if this idea will work. This effort is the initial stage of the TPAD data acquisition software; it is currently called TPADsys (TPAD integrated System).

The TPADsys is coded with Microsoft VC++6.0, plus all the dynamic links from National Instruments. The current version of TPADsys collects the following signals:

- three channels of GPR data (includes DMI),
- 1394 Real time video with resolution of 640X480,
- a max of eight channels of TPAD signals, accelerometers or others from the TPAD (Collection rate is 500 Hz), and
- GPS device (rate is one reading every second).

The GPR, DMI, and GPS signals are generated from the simulator software loaded on a second computer. Six TPAD signals are from the output from the vibration device (see Figure 5.2). Another two channels are from a function generator that controls the frequency of dynamic loading applied by the loading rollers. Figure 5.4 is the screen shot of TPADsys while it is collecting data. These data are available in real time during data collection.

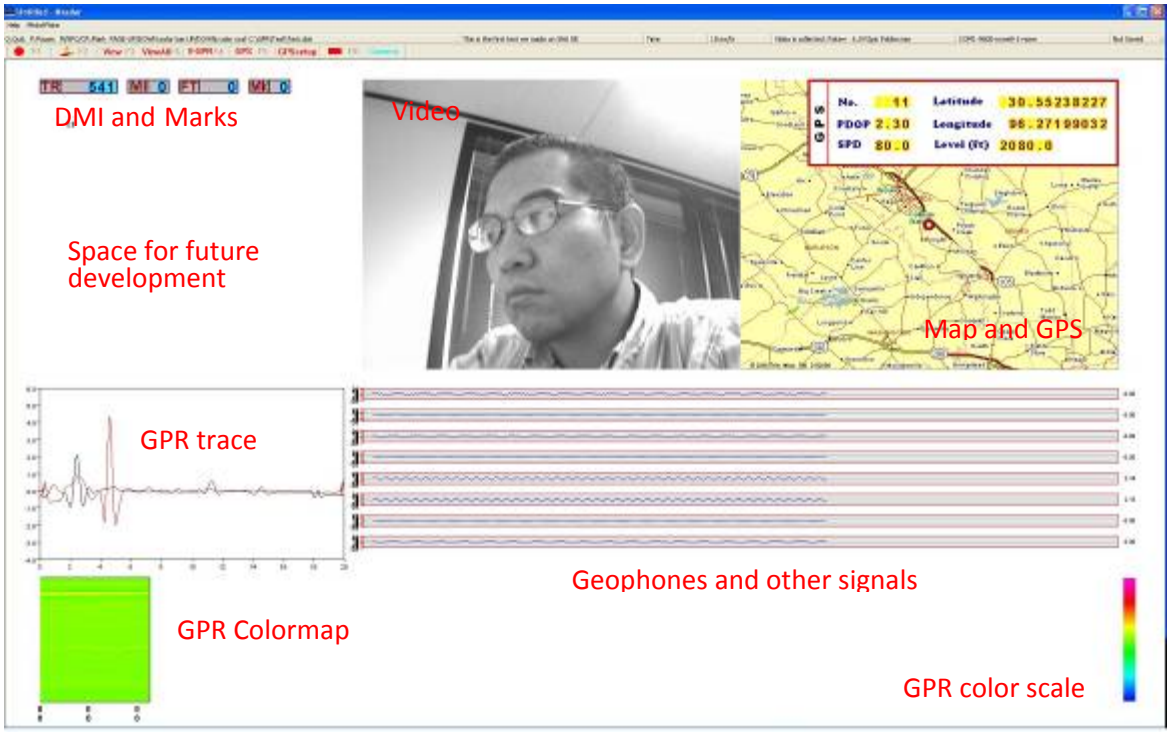

Figure 5.4: Screen Shot of the Prototype TPADsys Data Acquisition System.

On this screen, the GPR trace and color coded maps are displayed in real time. The map and GPS readings are in the top right corner of the screen. The current location is automatically marked on the map by a red circle. DMI and the marker count identify the current location and number of marks generated from the DMI output (which are located in the top left corner). The empty space under the DMI bar will be used for future development, but this will most probably have vehicle information provided by the manufacturer, typically vehicle speed, direction of travel, load levels, etc.

Figure 5.5 gives another screen shot showing the real-time signals from the GPR system, geophones, and other signals. This screen only shows the analog signals from the data acquisition card. The operator can use this display to check if all the sensors are working correctly.

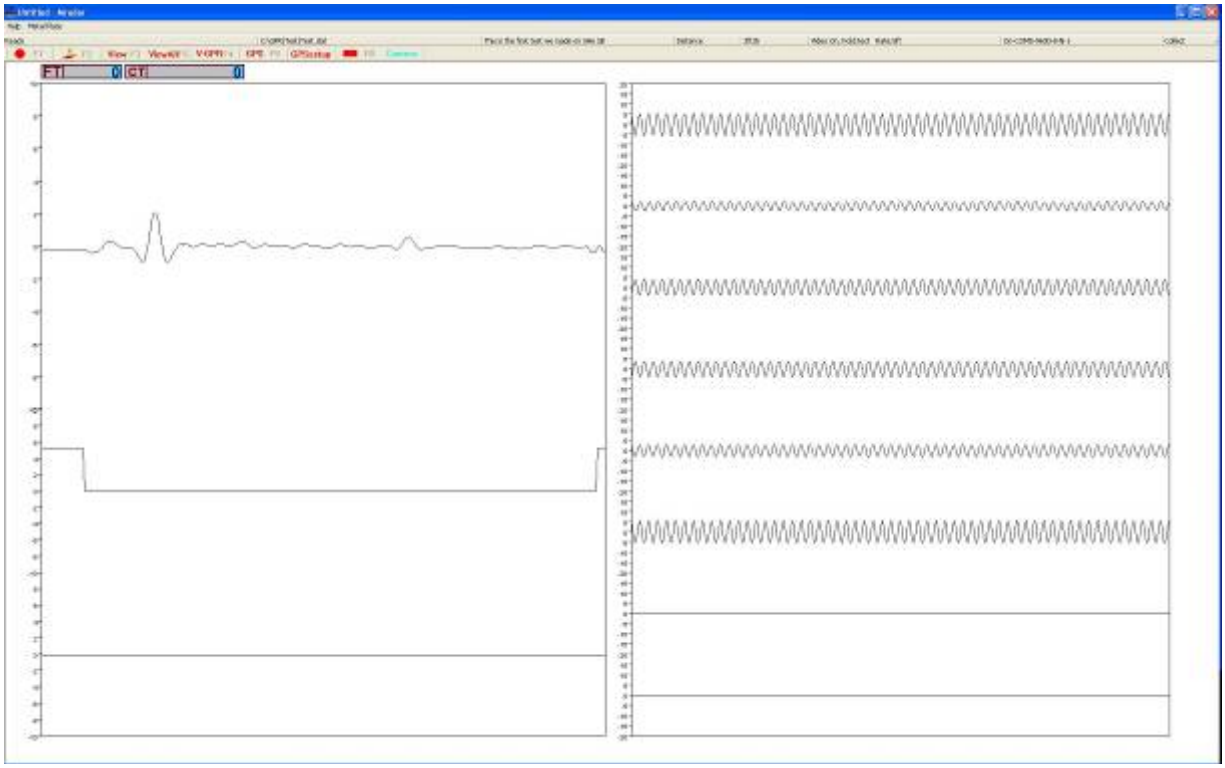

Figure 5.5: Another Screen Shot of the TPADsys.

Because this is the first version of the TPAD project data acquisition software, there are the following limitations and/or drawbacks to this program:

- Data are just collected and displayed on the screen and are not currently saved,
- Eight channels perhaps are not enough for the geophones and other signals, and
- Interface and screen need further improvements, but this is the first version.

Chapter 6. TPAD Data Acquisition Hardware Setup

6.1 Introduction

In the first year, we purchased all of the hardware required for the TPAD data acquisition system. Because this project involves activities of several organizations, the data acquisition system, developed by TTI, will ultimately be installed in the manufacturer's vehicle, and also needs to be hooked up with all signal outputs from the CTR rolling sensors and the TPAD manufacturer's accelerometers/distance/speed sensors. In this chapter, we give detailed information about the TPAD data acquisition hardware. Table 6.1 is the hardware list and some useful detailed technical information about each component.

The hardware listed in Table 6.1 includes items already purchased and these will be installed in the TPAD vehicle in the future. Several additional items will be required for the complete TPAD system. These items include the following:

- Ground penetration radar (GPR) system that is not yet purchased (potentially will use an existing Wavebounce unit available at TTI),
- CTR and the TPAD manufacturer will be in charge of all electronics before their signals enter TTI's data acquisition system (ultimately connected to NI-USB 6218 DAQ card as listed in Table 6.1),
- GPS antenna model, GA530, will be installed on the top of the TPAD vehicle (this item is not listed in the table), and
- DMI signal will be supported by the TPAD manufacturer (their DMI pulse will be connected to NI-USB 9215A DAQ card as in Table 6.1).

Figure 6.1 illustrates the location of some of the data acquisition components. On the front top of the vehicle, the camera will be installed using a strong magnet base plate for easy removal and repositioning. On the top of the loading system, the GPS antenna will be installed; it should be at least 3 feet above the vehicle for better reception. The box that holds the two data acquisition cards will be installed under the vehicle passenger's seat. The computer is panel mounted in front of the passenger for operating the data acquisition system. Most of the operations can be conducted by touching the screen. A compact keyboard will need to be installed for inputting header and other information.

Figure 6.2 shows the panel mount computer (model: VTPC170P) dimensions. Figure 6.3 shows all the interface connections of this computer. On the front of the computer, there are still two extra USB 2.0 ports.

Table 6.1: TPAD Data Acquisition System Hardware List

Name	Functions
NI-USB 9215A (BNC) DAQ card for GPR	4 channels of 16-bit simultaneously sampled analog input connected by BNC. Plug-and-play connectivity via USB, Sampling rates at 100 kS/s per channel Dimension: (5.54, 3.47, 1.0 in), Power consumption from USB 500 mA, max. Used for DMI and GPR data acquisition
NI-USB 6218 (BNC) DAQ card for other signals	16 differential BNC analog inputs (16-bit, 250 kS/s), Maximum voltage range is -10 to +10V 2 BNC analog outputs (16-bit, 250 kS/s); 8 digital inputs; 8 digital outputs; two 32-bit counters 60 V, CAT I isolation (1000 Vrms, 5 s withstand); locking USB cable; security cable slot NI signal streaming for sustained high-speed data streams over USB; Dimension: (9.25, 4.40, 2.50 in), powered by USB port, Maximum power requirement is 500ma at 5V
Panel Mount Computer Model: VTPC170P DAQ control computer	Resistive Touch Screen good for industry control purpose. Powerful 2.16 GHz Intel Dual Core T3400 processer Intel ®GME965 GMCH Gen4 integrated graphics 17" SXGA TFT LCD **Resolution:** 1280 x 1024, **Power Input:** 90-240V AC , 51W 2 RS-232 COM port, 2 LAN ports, 4 USB 2.0, 2 x IEEE 1394a Weight: 19 lb
GPS SPS351 DGPS/Beacon receiver	Horizontal accuracy: ±(0.25m + 1 ppm) RMS ±(0.8 ft + 1 ppm) Vertical accuracy: ±(0.50m + 1 ppm) RMS ±(1.6 ft + 1 ppm) Antenna: L1, GPS, MSK Beacon, SBAS Model: GA530 Dimensions (L × W × D) (9.4 in) × (4.7 in) × (1.9 in) 10.5 V to 28 V DC external power input, 4.5 W at 18 V in rover mode
IEEE1394b Firewire Camera Model:CSFS20CC2	IEEE1394.b interface (800Mbps) and quick delivery Color 1280(H) x 960(V) SXGA Dimension:1.73x1.14x1.73 in 20fps at SXGA, higher at lower resolutions Power: 8 to 30V DC (100mVpp ripple), max. 325mA via IEEE1394 cable, max. 2.6W Protocol: IIDC 1394-based digital camera specification Ver.1.31 compliance Lens connection: ½ inches CCD, C type mount

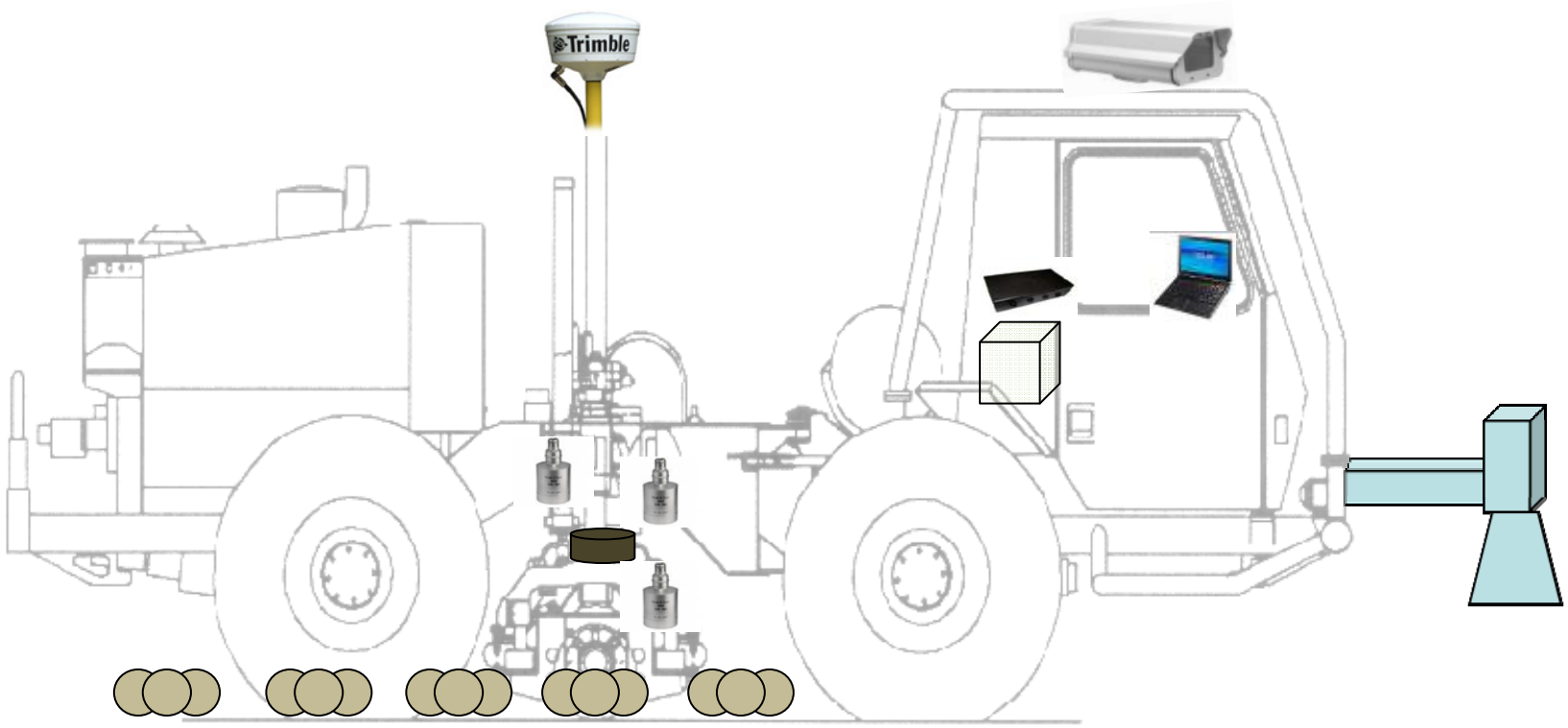

Figure 6.1: TPAD Data Acquisition System Hardware Setup

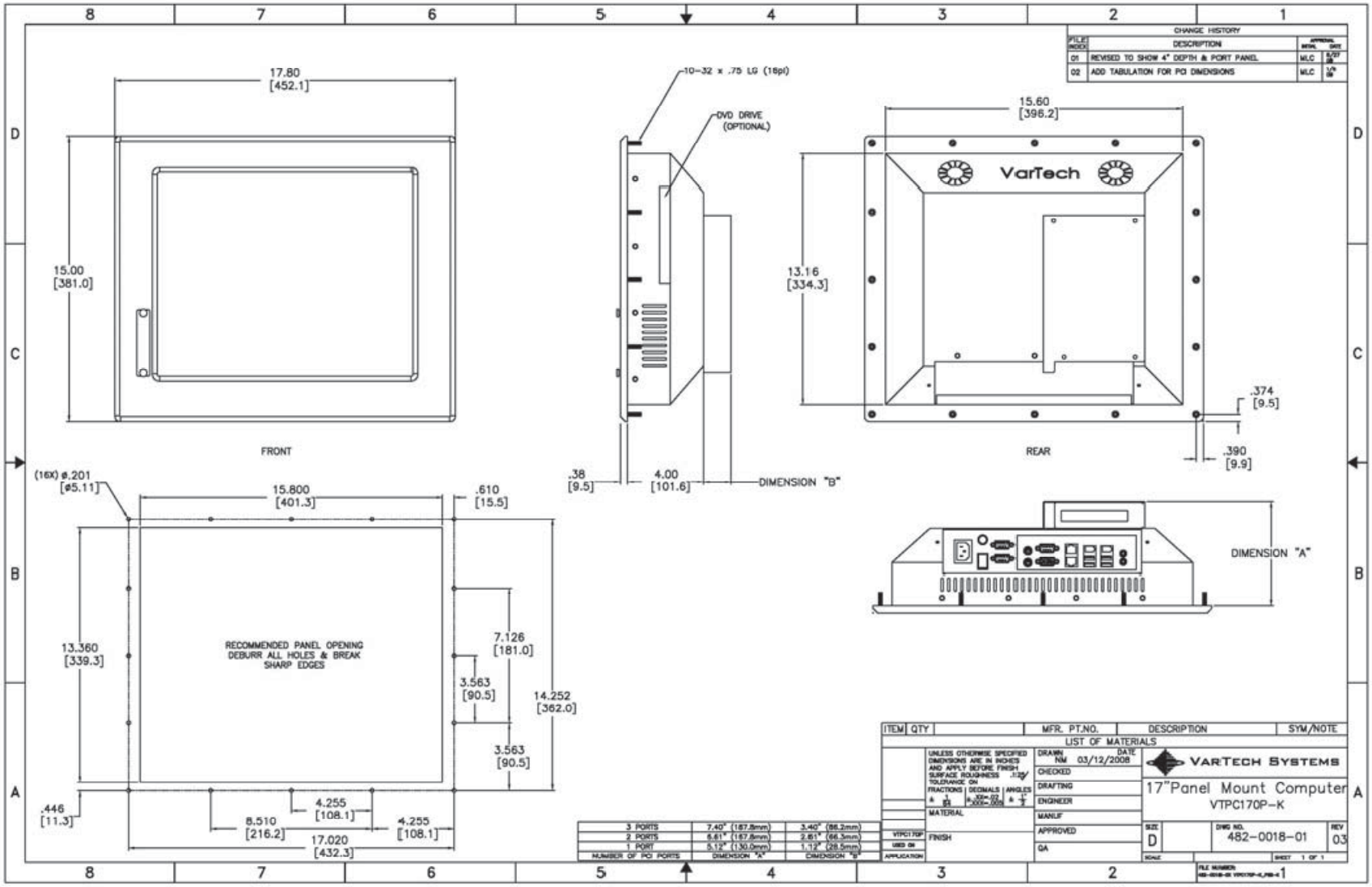

Figure 6.2: Panel Mount Computer: VTPC170P Dimension

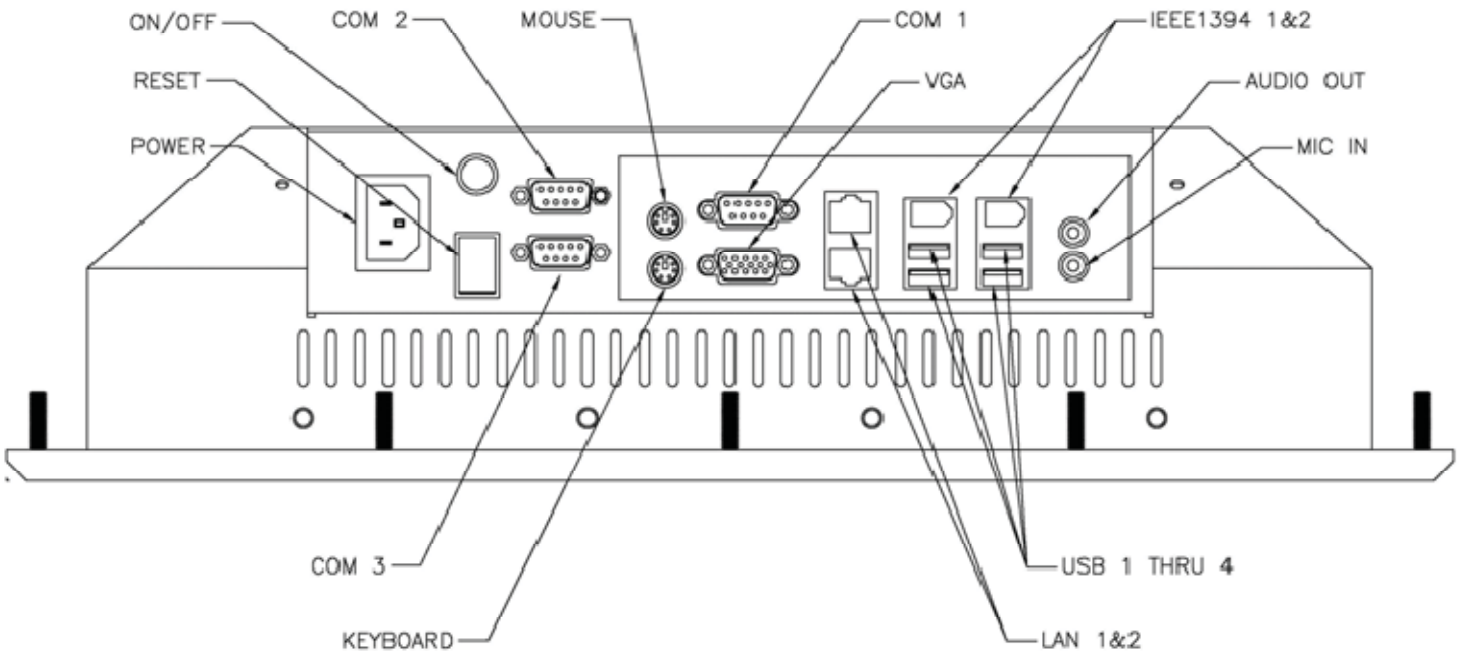

Figure 6.3: Panel Mount Computer: VTPC170P Interface

6.2 Power Supply Equipment for the Data Acquisition System

Table 6.2 lists the power requirements for the data acquisition system. In this table, the GPR unit's power estimate is based on existing units. From this table, note that two data acquisition cards and firewire camera are powered by the computer directly. The GPS unit needs 10.5~28VDC power supply and is powered by a DC power adapter (supplied by Trimble). This power adapter needs 110VAC power supply. So at a minimum the TPAD needs a 260W 110AC power supply. For safety reasons, we can add 75% extra power and the recommended power requirement is 450W @ 110VAC. This calculation does not include power requirements for components supplied by the TPAD manufacturer and CTR.

Table 6.2: TPAD Data Acquisition System Power Requirement

Name	Power Requirement Description	Power Solution	Power Consume
NI-USB 9215A(BNC)	5V from USB 500 mA max	From computer USB	3.0W
NI-USB 6218 (BNC)	5V powered by USB port, Maximum power requirement is 500ma at 5V	From computer USB	3.0W
Panel Mount Computer	90-240V AC, 51W	From Vehicle 110VAC power supply	51W
GPS SPS351	10.5 V to 28 V DC external power input, 4.5 W at 18 V in rover mode	Has separate power adapter, adapter need 110AC	4.5W
Firewire Camera	Power: 8 to 30V DC (100mVpp ripple), max. 325mA via IEEE1394 cable, max. 2.6W	From computer's firewire port	2.6W
GPR Unit	110VAC 200VA or W	From vehicle's 110VAC power supply	200W
Total			264.1W

6.3 Space Consideration for the Data Acquisition System

The space inside the TPAD vehicle will be limited. The data acquisition components will be made as compact as possible. We purchased a storage box (made from ABS/PC Blended Plastic; color is light gray) for housing the two DAQ cards, GPS controller, the cables, and other power adapter. Figure 6.4 is a photo of the box. Many holes will be drilled for the access of all required cables when this enclosure is installed in the vehicle.

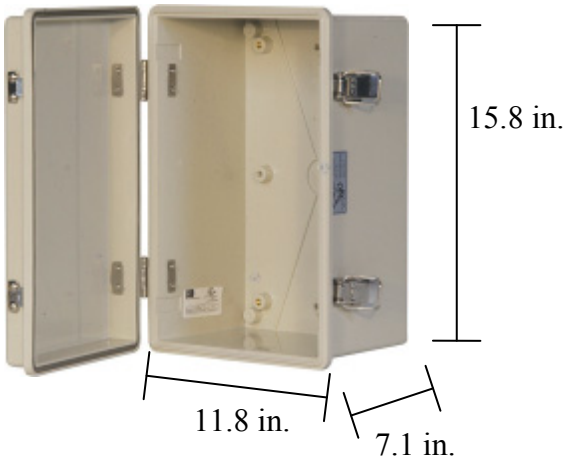

Figure 6.4: Dimension of the Storage Box

The proposed dimensions inside the TPAD vehicle cab are shown in Figure 6.5. Between the operator and passenger seats, there is sufficient space to install the electronic components. Figure 6.6 shows the proposed layout for the TPAD data acquisition system setup inside vehicle. The GPR controller box will face forward for easy adjustment when testing. The storage box will be located behind the GPR control box. Most of the wires are hidden inside this enclosure box. A steel or aluminum frame is built to support the panel mount touch screen computer on the top of the other components. The tilt angle of the computer can be adjusted for best view. The computer can also be flipped away from top for easy access to the enclosure below. Under the computer, a compact keyboard can be installed for input.

The GPR control box is 19 in. wide, 2 in. high, and 14 in. deep. If the Wavebounce system is used, the control box may be re-packaged to a smaller size. Dimensional details of the computer is presented in Figure 6.2. Inside the cable duct between the computer and the storage box, there are the following cables:

- USB cable for NI-USB 9215A,
- USB cable for NI-USB 6218,
- Computer 110VAC power cable,
- Serial port or COM port cable, and
- 1394 Firewire camera cable.

During field testing, the camera housing needs be positioned on the top of the vehicle cab. After completing the test, the camera package should be stored inside the vehicle to prevent the damage due to rain or other sources of moisture.

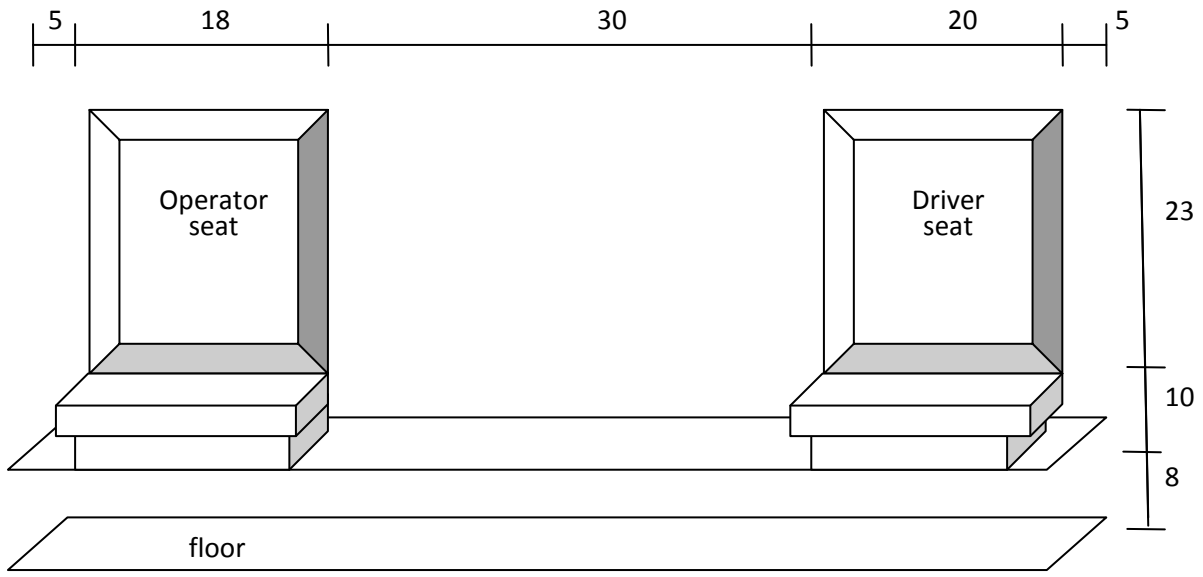

Figure 6.5: TPAD Big Cab Dimensions Measurement (Units in Inches)

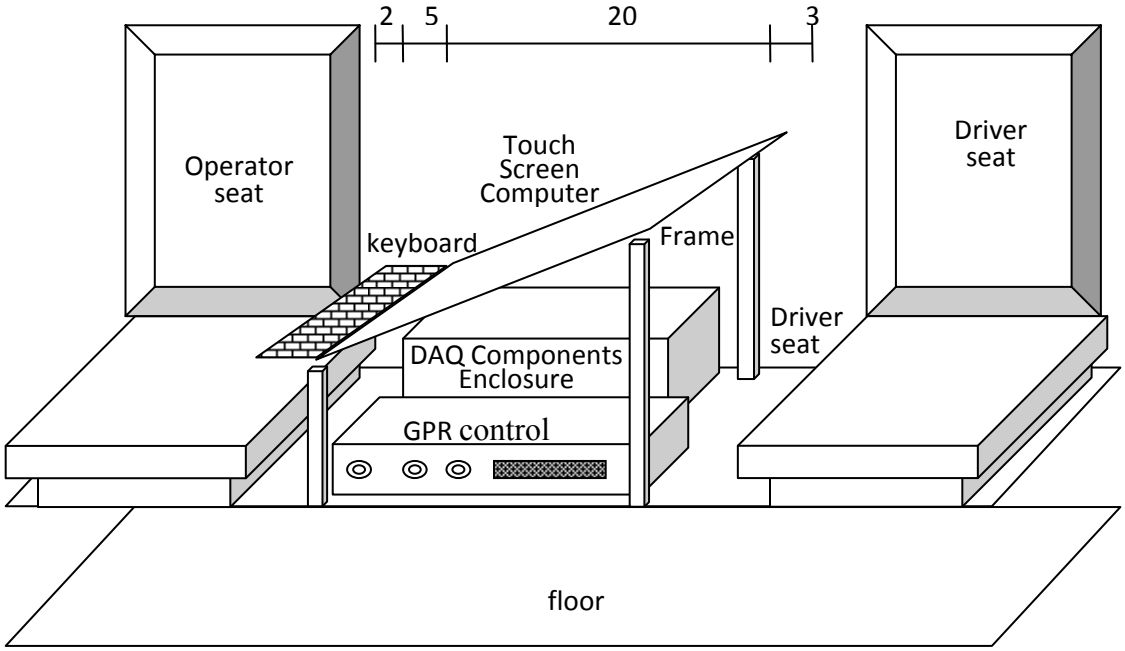

Figure 6.6: Proposed Layout for the TPAD Data Acquisition System Setup inside Vehicle (Unit in Inches)

6.4 Photos of All the Purchased Hardware for the DAQ System

The equipment purchased by TTI and the electronic components are shown in Figures 6.7 to 6.17. While some are used solely in the development of the TPAD data acquisition system, most will ultimately be installed into the new TAPD vehicle.

Figure 6.7: Panel Mount Computer (Model: VTPC170P)

Figure 6.8: Panel Mount Computer Back View (Model: VTPC170P)

Figure 6.9: NI-USB 9215A(BNC) DAQ Card for GPR

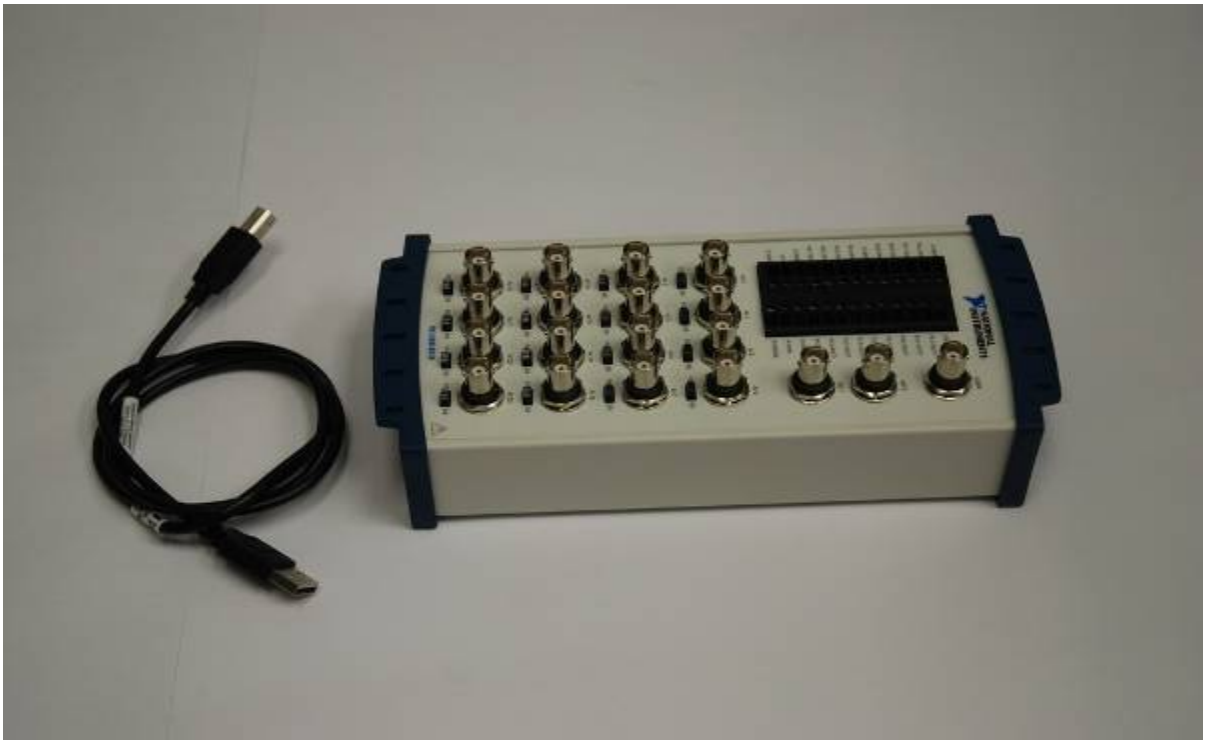

Figure 6.10: NI-USB 6218 (BNC) DAQ Card

Figure 6.11: GPS SPS351 DGPS/Beacon Receiver, Antenna, and Power Adapter

Figure 6.12: NI-cDAQ-9172 Carrier and NI-9263 Analog Output DAQ Card for Simulator

Figure 6.13: IEEE1394b Firewire Camera (Model: CSFS20CC2)

Figure 6.14: TPAD Geophones Simulator Device (Home Made)

Figure 6.15: Enclosure for Housing DAQ Cards and GPS Unit

Figure 6.16: Oscilloscope and Function Generator

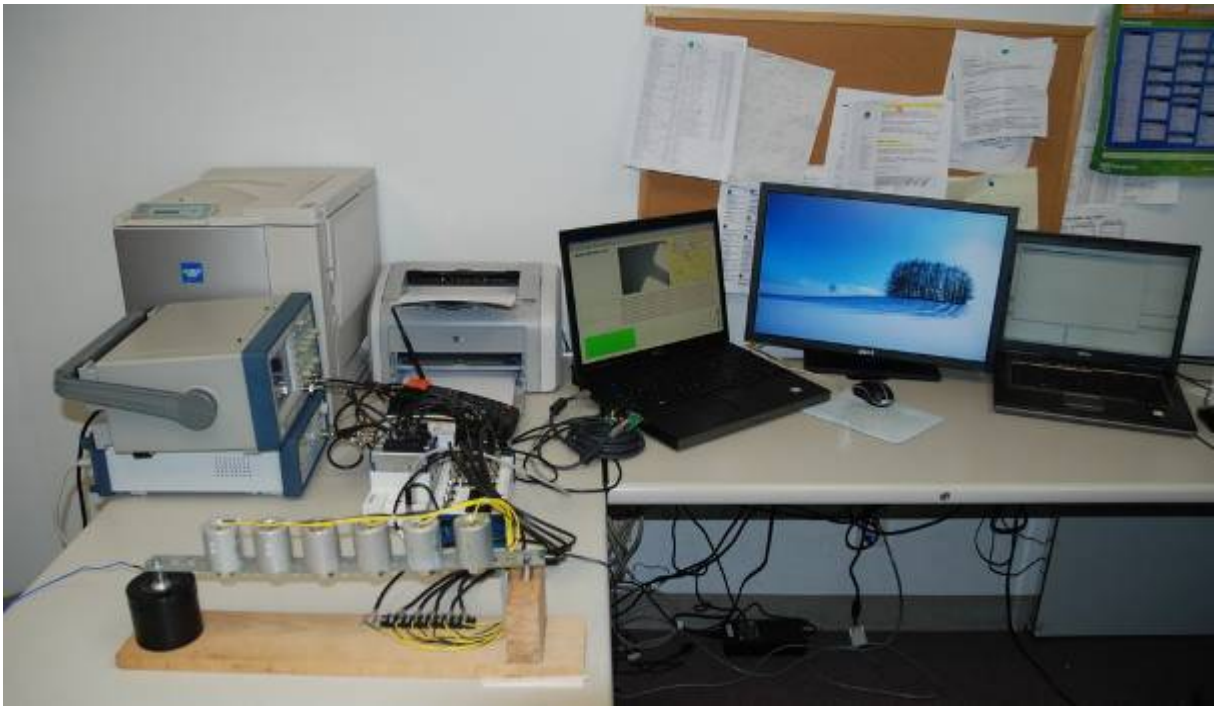

Figure 6.17: System Development Lab Simulation Work Space for This Project

Chapter 7. Activities in Year 2

7.1 Path Forward

The activities during Year 1 have been very productive and have allowed the path forward to be well defined. In Year 2, the primary activities can be summarized as follows.

1. Construction of the TPAD Vehicle
   Specifications for the TPAD moving platform and associated RDD function will be developed. With approval from the PMC, a request for proposal (RFP) will be issued by UT, a manufacturer will be selected, and construction of the vehicle will be completed.

2. Construction of New Rolling Sensors
   Concurrent with developing the specifications and construction of the TPAD, new RDD rolling sensors will be developed that will function properly at speeds of 5 mph and above. The sensors will undergo test trials with the UT RDD using the pavement testbed at the TxDOT Flight Services Facility (FSF) before installation in the TPAD.

3. Initial Tests of the Integrated Data Acquisition and Display System
   The first-generation integrated data acquisition system will undergo field trials using the UT RDD at the FSF. This work will likely be conducted with a limited number of additional functions in operation (such as GPR and GPS). With the results from the field trials, work will commence on any changes or upgrades needed to develop the final data integration and display system.

Although the overall project is somewhat behind schedule, the opportunity to perform field tests with the prototype ivi RDD was extremely valuable in developing reasonable specifications for our final design. The unknowns were significantly reduced by the field tests and a better TPAD will be developed and constructed in a more timely manner. As such, the project should gain some time and come closer to the original schedule.

References

Christensen, E., personal communication, Industrial Vehicles Inc., Austin, July 29, 2009 during RDD Demo at TxDOT Flight Facility Site at the Austin Bergstrom International Airport.

Lee, L. J., "Improved Rolling Dynamic Deflectometer Testing and Analysis Procedures," Ph.D. Dissertation, University of Texas at Austin, 2006.

Bay, J. A., and K. H. Stokoe, II, "Development of a Rolling Dynamic Deflectometer for Continuous Deflection Testing of Pavements," Publication FHWA/TX-99/1422-3F, FHWA/Texas Department of Transportation, Austin, Texas, May 1998.